Bone histomorphometric analysis of the proximal tibia showed that bone formation rate (BFR/BS) and the osteoblast surface (Ob.S/BS) were significantly decreased in both female and male AtmKO mice (Fig. 2). The osteoclast surface (Oc.S/BS) was also reduced in the KO mice, suggesting that both bone formation and resorption were suppressed in AtmKO mice and that the observed osteopenic phenotype was caused mainly by impaired bone formation.

Cellular basis of impaired bone formation

To determine whether impaired bone formation was due to a cell autonomous defect, in vitro osteoblastogenesis assays were performed. The number of CFU-F (Fig. 3A), CFU-ALP (Fig. 3B), and CFU-OB (data not shown) were significantly reduced in the bone marrow of AtmKO mice. The decrease in CFU-F, which reflects the number and/or proliferative potential of mesenchymal progenitors, suggested that the defect was not specific to the osteoblastic lineage but involved other lineages as well. In fact, the number of CFU-adipocyte was also reduced (data not shown). We performed osteoblastogenesis assays in the presence of *N*-acetyl cysteine (NAC) to reduce oxidative stress, which often affects cell proliferation and induces senescence of primary cultured murine cells. As shown in Figs. 3A and B, supplementation with NAC increased the number of CFU-F and CFU-ALP in bone marrow cultures from control mice, but not in cultures from AtmKO mice. Notably, the ratio of CFU-ALP to CFU-F was not markedly altered between the genotypes, suggesting that differentiation, especially the ability to differentiate into osteoblasts, was not impaired in AtmKO mice.

To address the question whether the absence of Atm affected the differentiation process, osteoblasts were isolated from calvarias of homozygous and heterozygous knockout mice and cultured in vitro. As shown in Fig. 3C, calvaria-derived osteoblastic cells differentiated at comparable levels, suggesting that the differentiation potential of osteoblasts was not impaired in AtmKO mice. Together, with results from the CFU assays, these data collectively suggested that the impaired bone formation was not due to a defect in the differentiation program of osteoblasts per se but to the proliferative potential of mesenchymal progenitors.

As for the hematopoietic lineage, M-CSF-dependent proliferation of bone marrow cells from AtmKO mice did not differ from that of control mice (Fig. 4A). When osteoclastogenic potential was assessed in bone marrow cultures with M-CSF and RANKL, neither the number of TRAP-positive multinucleated cells formed (Fig. 4B) nor their morphology (Fig. 4C) differed between the genotypes.

Reduced IGF1 receptor with activation of p38 in Atm-deficient marrow stromal cells

To gain some insight into the molecular mechanism underlying the impaired proliferation of mesenchymal progenitors in AtmKO mice, the expression of molecules involved in ATM signaling was analyzed by immunoblotting. As shown in Fig. 5 (right lane), the level of phosphorylated p38MAPK (P-p38) was elevated in marrow stromal cells derived from AtmKO mice, while the total amount of p38 in the experimental and control cultures did not differ. By contrast, the expression of IGF-I receptor (IGF1R) was markedly reduced in AtmKO-derived marrow stromal cells compared with control cells (Fig. 5A). The level of Abl, a downstream effector molecule involved in the ATM pathway, did not differ between the genotypes. Next, we determined whether the IGF response was impaired in cells derived from AtmKO mice. As shown in Fig. 5B, control cells responded to IGF with increased proliferation, whereas the response to IGF was severely impaired in the stromal cells from AtmKO mice, suggesting that a decline in the expression level of IGF1R causes IGF-dependent proliferation in AtmKO mice.

Discussion

In the present study, we demonstrate that AtmKO mice show reduced bone formation due to a proliferative defect in

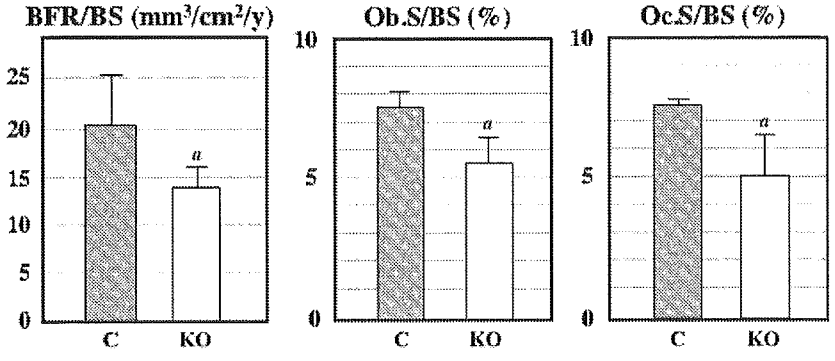

Fig. 2. Bone histomorphometric analysis of AtmKO mice. Decreases in bone formation rate (BFR/BS, left), osteoblast surface (Ob.S/BS, center), and osteoclast surface (Oc.S/BS, right) were measured from the proximal tibias of male AtmKO (KO) mice and compared with heterozygous (C) littermate controls. Data expressed are the means ± SD. $^{a}P < 0.05$, significantly different from the respective heterozygous control group.

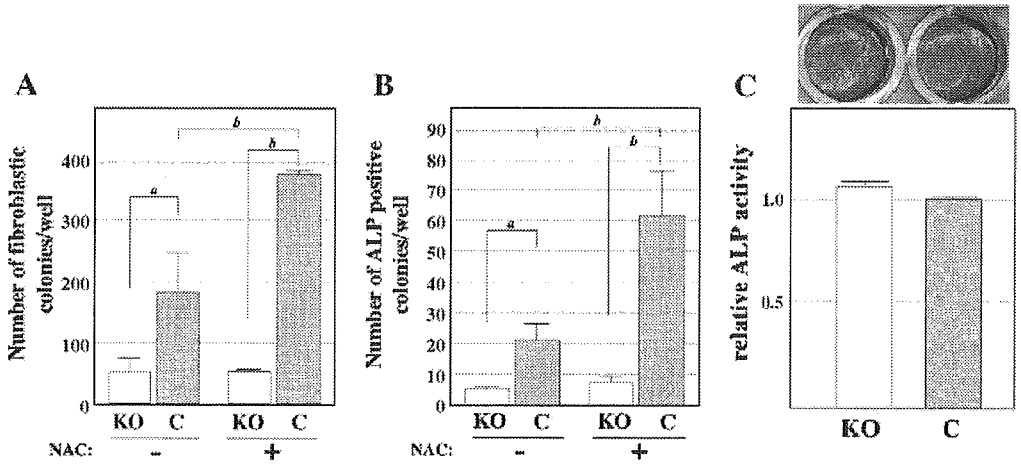

Fig. 3. Colony formation assay of bone marrow cells and calvarial osteoblast differentiation. (A) CFU-F in bone marrow cells derived from AtmKO (KO) or littermate wild-type or heterozygous control (C) mice ($n = 3\sim5$) are shown. (B) CFU-ALP. Note the significant reductions in both CFU-F and CFU-ALP ($P < 0.05$, KO versus control). *N*-acetyl cysteine (NAC, 10 mM) improved the numbers of CFU-F and CFU-ALP in control but not in cells from AtmKO mice. (C, upper panel) A representative photograph of the wells stained for ALP activity. Lower panel, relative ALP of calvarial cell cultures. No significant difference in morphology or ALP activity was observed between knockout (KO) and controls (C). Data represent the means ± SD. $^{a}P < 0.05$ and $^{b}P < 0.005$, significantly different from the respective control group. No significant difference was detected in the presence or absence of NAC in KO cells either in CFU-F or CFU-ALP assays.

mesenchymal progenitor cells, in addition to other age-related disorders observed in the human syndrome, AT, including neurodegeneration, immune defects, tumor formation, and genomic instability [7–9]. It has been suggested that, in mice as well as in humans, age-related decline in osteoblast number and function is caused by a decrease in number and proliferative potential of mesenchymal stem cells [16–19]. AtmKO mice recapitulate these cellular defects as early as 10 weeks of age. At this age, there are no signs of lymphoma or severe growth retardation in KO mice [7], suggesting that the bone phenotype is not caused by the secondary effects of those defects. The difference in bone mass between genotypes was more pronounced with age. The loss of bone mass associated with age may be accelerated by other abnormalities, such as growth retardation, lymphoma, immune defects, and cachexia. Importantly, we have shown in this study that the bone marrow cells exhibited a cell autonomous defect in proliferation. Therefore, it is suggested that the impairment in bone formation with a proliferative defect in bone marrow stem cells causes the osteopenic phenotype in AtmKO mice, although we cannot exclude the possibility that the defects such as T-lymphopenia and hypogonadism affected the bone phenotype of more aged mice. The microstructural alterations in the lumbar vertebrae of AtmKO mice are also similar to those observed in naturally aging C57BL/6J mice [20]. Thus, AtmKO mice may provide a suitable model to study the pathophysiology of senile osteoporosis without the necessity of raising them for 2 to 3 years.

Recently, Bonyadi et al. reported that Sca1 KO mice develop an age-dependent osteopenia [21]. Sca1 KO mice exhibit a decrease in the number of osteoprogenitors as well

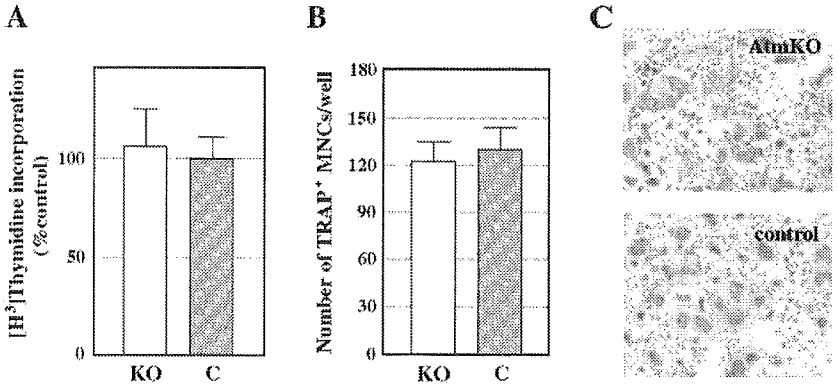

Fig. 4. M-CSF-dependent proliferation and in vitro osteoclastogenesis of bone marrow cells. (A) No obvious difference in M-CSF-dependent [^{3}H]thymidine incorporation into bone marrow cells was detected. (B) The number of multinucleated TRAP-positive cells derived from bone marrow cells in the presence of RANKL and M-CSF. No significant difference between the cells from AtmKO (KO) and littermate control (C) mice was observed. (C) TRAP staining of the in-vitro-generated multinucleated cells.

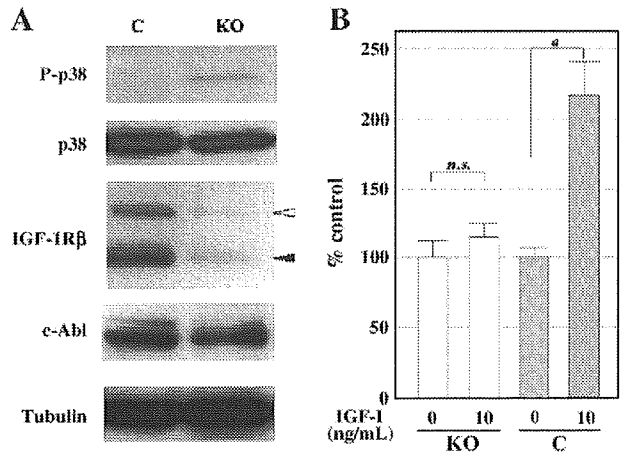

Fig. 5. Expression analysis of IGF-1 receptor in bone marrow cells. (A) Total cell lysates of bone marrow stromal cells from wild-type (C, left lane) or Atm knockout (KO, right lane) were subjected to immunoblot analyses. Top panel (P-p38), activated (phosphorylated) p38. Second panel (p38), total p38 MAP kinase. The activated p38 is only detected in AtmKO. These two panels were from a membrane blot. Third panel (IGF-IRβ), probed with antibody against the insulin-like growth factor receptor β subunit. The upper (open arrowhead) and lower (closed arrowhead) bands correspond to unprocessed and processed β subunit protein, respectively. Fourth panel (c-Abl) shows expression level of c-Abl protein. The bottom panel, probed with anti-tubulin antibody to control for protein loading in the last three panels (IGF-IRβ, c-Abl). (B) IGF-I response. Bone marrow stromal cells from Atm knockout (KO) or wild-type (C) were cultured with or without IGF-I. Incorporated thymidine was measured and displayed as fold change (%) compared to culture without IGF for each genotype. $^{a}P < 0.005$; n.s., not significant.

as CFU-F and have a non-cell autonomous defect in osteoclasts [21]. Although defects of osteoblasts and osteoclasts are similarly observed in AtmKO mice, the expression of Sca1 mRNA was not altered in AtmKO mice (data not shown). Additionally, the onset of the bone phenotype in Sca1 KO (~12 months of age) was very late, compared with that of AtmKO mice (~10 weeks). Thus, the impact of ATM deficiency on bone formation was more severe than that of Sca1 deficiency.

It has been reported that AtmKO mice showed reduced numbers of leukocytes in the circulation as well as bone marrow [7–9,22]. Although osteoclast surface was reduced in the bone of AtmKO mice, osteoclastogenic potential as well as M-CSF-dependent cell proliferation in vitro was normal, pointing to the involvement of impaired ability of the marrow environment to support proliferation/differentiation of osteoclast progenitors rather than cell autonomous dysfunction in the hematopoietic lineage. Concerning the osteoblastic lineage of AtmKO mice, the defect lies mainly in CFU-F, while the differentiation of osteoblasts was rather normal. Thus, it is tempting to speculate that multi-potent stem or progenitor cells are more sensitive to Atm deficiency than are differentiated cells. As we did not find any difference in the expression of Jagged-1 (data not shown), one of the key molecules that function in the bone marrow niche [23], the molecular defect in niche function of AtmKO mice remains to be clarified.

Chk2 is a checkpoint kinase that functions downstream of ATM and phosphorylates p53 to stabilize it [11,24]. Soft X-ray analysis of bones from Chk2 KO mice [25] revealed no alteration in bone density (AH et al., unpublished observation). It has been reported that the bones of mice lacking p53, the target of ATM and Chk2 kinases, were normal, although they were resistant to bone loss in response to unloading [26]. Thus, it is unlikely that the Chk2 pathway is involved in the impaired bone formation in AtmKO mice.

It has been reported that mice lacking Abl, another downstream kinase of ATM, exhibit an osteopenic phenotype due to reduced bone formation, which is caused mainly by a defect in osteoblast differentiation [27]. In AtmKO mice, by contrast, osteoblastic differentiation is normal. Li et al. have recently demonstrated distinct roles for ATM and Abl in the oxidative stress response and that ATM and Abl differentially regulate osteoblast expression of PKCδ [28]. We demonstrated that the improved colony formation following supplementation with NAC was diminished in AtmKO-derived cultures. Thus, the possibility exists that irreversible damage by oxidative stress had already altered the proliferative potential of AtmKO-derived progenitor cells or that an additional molecular defect(s), other than the oxidative stress response, is involved.

IGF plays important roles in bone growth and metabolism [29–31]. This has been supported by genetic approaches in mice [32–35]. *ATM* deficiency downregulates the transcription of the *IGF1R* gene [36], and we found, in fact, that the expression of IGF1R, as well as the responsiveness to IGF, was decreased in marrow stromal cells of AtmKO mice. These results indicate that defective IGF signaling may be involved in the impaired bone formation observed in AtmKO mice. In addition, since serum deprivation induces oxidative stress, due mainly to loss of IGF [37], the connection between IGF activity and oxidative stress may be an interesting relationship warranting further investigation.

In conclusion, we demonstrate that AtmKO mice present an osteopenic phenotype as early as 10 weeks, apparently due to decreased bone-marrow-derived mesenchymal progenitors. This decline in mesenchymal progenitors may be the result of decreased expression of IGF1R, an important regulator of proliferation. The AtmKO mouse model may be a useful tool for further studies of senile osteoporosis.

Acknowledgments

The authors thank Drs. Yoshiko Masuda and Aya Sasaki for technical assistance in bone analyses; Miho Kamiya, Makiko Matsuura, and Kumi Tsutsumi for in vitro experiments and genotyping; Dr. Kazuhito Naka for advise in analyses of protein expression; and Dr. Akira Matsuura for critical reading of the manuscript. This study was supported in part by a grant from the Program for Promotion of Fundamental Studies in Health Sciences of the Organiza-

tion for Pharmaceutical Safety and Research of Japan and by a Research Grant for Longevity Sciences from the Ministry of Health, Labor and Welfare.

References

[1] Bilezikian JP, Raisz LG, Rodan GA, editors. Principles of bone biology. San Diego, CA: Academic Press; 2002.
[2] Favus MJ, editor. Primer on the metabolic bone diseases and disorders of mineral metabolism. American Society for Bone and Mineral Research; 2003.
[3] Hasty P, Vijg J. Accelerating aging by mouse reverse genetics: a rational approach to understanding longevity. Aging Cell 2004;3:55–65.
[4] Tyner SD, Venkatachalam S, Choi J, Jones S, Ghebranious N, Igelmann H, et al. p53 mutant mice that display early ageing-associated phenotypes. Nature 2002;415:45–53.
[5] Kuro-o M, Matsumura Y, Aizawa H, Kawaguchi H, Suga T, Utsugi T, et al. Mutation of the mouse klotho gene leads to a syndrome resembling ageing. Nature 1997;390:45–51.
[6] Lavin MF, Shiloh Y. The genetic defect in ataxia-telangiectasia. Annu Rev Immunol 1997;15:177–202.
[7] Barlow C, Hirotsune S, Paylor R, Liyanage M, Eckhaus M, Collins F, et al. Atm-deficient mice: a paradigm of ataxia telangiectasia. Cell 1996;86:159–71.
[8] Elson A, Wang Y, Daugherty CJ, Morton CC, Zhou F, Campos-Torres J, et al. Pleiotropic defects in ataxia-telangiectasia protein-deficient mice. Proc Natl Acad Sci U S A 1996;93:13084–9.
[9] Xu Y, Ashley T, Brainerd EE, Bronson RT, Meyn MS, Baltimore D. Targeted disruption of ATM leads to growth retardation, chromosomal fragmentation during meiosis, immune defects, and thymic lymphoma. Genes Dev 1996;10:2411–22.
[10] Rotman G, Shiloh Y. ATM: from gene to function. Hum Mol Genet 1998;7:1555–63.
[11] Shiloh Y. ATM and related protein kinases: safeguarding genome integrity. Nat Rev Cancer 2003;3:155–68.
[12] Liao MJ, Van Dyke T. Critical role for Atm in suppressing V(D)J recombination-driven thymic lymphoma. Genes Dev 1999;13:1246–50.
[13] Shibata T, Shira-Ishi A, Sato T, Masaki T, Masuda A, Hishiya A, et al. Vitamin D hormone inhibits osteoclastogenesis in vivo by decreasing the pool of osteoclast precursors in bone marrow. J Bone Miner Res 2002;17:622–9.
[14] Jilka RL, Weinstein RS, Takahashi K, Parfitt AM, Manolagas SC. Linkage of decreased bone mass with impaired osteoblastogenesis in a murine model of accelerated senescence. J Clin Invest 1996;97:1732–40.
[15] Jochum W, David JP, Elliott C, Wutz A, Plenk Jr H, Matsuo K, et al. Increased bone formation and osteosclerosis in mice overexpressing the transcription factor Fra-1. Nat Med 2000;6:980–4.
[16] Tsuji T, Hughes FJ, McCulloch CA, Melcher AH. Effects of donor age on osteogenic cells of rat bone marrow in vitro. Mech Ageing Dev 1990;51:121–32.
[17] Kahn A, Gibbons R, Perkins S, Gazit D. Age-related bone loss. A hypothesis and initial assessment in mice. Clin Orthop 1995:69–75.
[18] Bergman RJ, Gazit D, Kahn AJ, Gruber H, McDougall S, Hahn TJ. Age-related changes in osteogenic stem cells in mice. J Bone Miner Res 1996;11:568–77.
[19] D'Ippolito G, Schiller PC, Ricordi C, Roos BA, Howard GA. Age-related osteogenic potential of mesenchymal stromal stem cells from human vertebral bone marrow. J Bone Miner Res 1999;14:1115–22.
[20] Halloran BP, Ferguson VL, Simske SJ, Burghardt A, Venton LL, Majumdar S. Changes in bone structure and mass with advancing age in the male C57BL/6J mouse. J Bone Miner Res 2002;17:1044–50.
[21] Bonyadi M, Waldman SD, Liu D, Aubin JE, Grynpas MD, Stanford WL. Mesenchymal progenitor self-renewal deficiency leads to age-dependent osteoporosis in Sca-1/Ly-6A null mice. Proc Natl Acad Sci U S A 2003;100:5840–5.
[22] Peter Y, Rotman G, Lotem J, Elson A, Shiloh Y, Groner Y. Elevated Cu/Zn-SOD exacerbates radiation sensitivity and hematopoietic abnormalities of Atm-deficient mice. EMBO J 2001;20:1538–46.
[23] Calvi LM, Adams GB, Weibrecht KW, Weber JM, Olson DP, Knight MC, et al. Osteoblastic cells regulate the haematopoietic stem cell niche. Nature 2003;425:841–6.
[24] Chaturvedi P, Eng WK, Zhu Y, Mattern MR, Mishra R, Hurle MR, et al. Mammalian Chk2 is a downstream effector of the ATM-dependent DNA damage checkpoint pathway. Oncogene 1999;18:4047–54.
[25] Takai H, Naka K, Okada Y, Watanabe M, Harada N, Saito S, et al. Chk2-deficient mice exhibit radioresistance and defective p53-mediated transcription. EMBO J 2002;21:5195–205.
[26] Sakai A, Sakata T, Tanaka S, Okazaki R, Kunugita N, Norimura T, et al. Disruption of the p53 gene results in preserved trabecular bone mass and bone formation after mechanical unloading. J Bone Miner Res 2002;17:119–27.
[27] Li B, Boast S, de los Santos K, Schieren I, Quiroz M, Teitelbaum SL, et al. Mice deficient in Abl are osteoporotic and have defects in osteoblast maturation. Nat Genet 2000;24:304–8.
[28] Li B, Wang X, Rasheed N, Hu Y, Boast S, Ishii T, et al. Distinct roles of c-Abl and Atm in oxidative stress response are mediated by protein kinase C delta. Genes Dev 2004;18:1824–37.
[29] Baylink DJ, Finkelman RD, Mohan S. Growth factors to stimulate bone formation. J Bone Miner Res 1993;8(Suppl. 2):S565–72.
[30] Delany AM, Pash JM, Canalis E. Cellular and clinical perspectives on skeletal insulin-like growth factor I. J Cell Biochem 1994;55:328–33.
[31] Hayden JM, Mohan S, Baylink DJ. The insulin-like growth factor system and the coupling of formation to resorption. Bone 1995;17: 93S–8S.
[32] Zhang M, Xuan S, Bouxsein ML, von Stechow D, Akeno N, Faugere MC, et al. Osteoblast-specific knockout of the insulin-like growth factor (IGF) receptor gene reveals an essential role of IGF signaling in bone matrix mineralization. J Biol Chem 2002;277: 44005–12.
[33] Devlin RD, Du Z, Buccilli V, Jorgetti V, Canalis E. Transgenic mice overexpressing insulin-like growth factor binding protein-5 display transiently decreased osteoblastic function and osteopenia. Endocrinology 2002;143:3955–62.
[34] Bikle DD, Sakata T, Leary C, Elalieh H, Ginzinger D, Rosen CJ, et al. Insulin-like growth factor I is required for the anabolic actions of parathyroid hormone on mouse bone. J Bone Miner Res 2002;17: 1570–8.
[35] Woitge HW, Kream BE. Calvariae from fetal mice with a disrupted Igf1 gene have reduced rates of collagen synthesis but maintain responsiveness to glucocorticoids. J Bone Miner Res 2000;15:1956–64.
[36] Peretz S, Jensen R, Baserga R, Glazer PM. ATM-dependent expression of the insulin-like growth factor-I receptor in a pathway regulating radiation response. Proc Natl Acad Sci U S A 2001;98:1676–81.
[37] Busiguina S, Fernandez AM, Barrios V, Clark R, Tolbert DL, Berciano J, et al. Neurodegeneration is associated to changes in serum insulin-like growth factors. Neurobiol Dis 2000;7:657–65.

Published Online First on March 3, 2006

DNase II and the Chk2 DNA Damage Pathway Form a Genetic Barrier Blocking Replication of Horizontally Transferred DNA

Anna Bergsmedh,[1] Jacob Ehnfors,[1] Kohki Kawane,[3] Noboru Motoyama,[2] Shigekazu Nagata,[3] and Lars Holmgren[1]

[1]Cancer Center Karolinska Hospital, Karolinska Institutet, Stockholm, Sweden; [2]Department of Geriatric Research, National Institute for Longevity Sciences, Obu, Aichi, Japan; and [3]Department of Genetics, Osaka University Medical School, Suita, Osaka, Japan

Abstract

We have previously shown that DNA from dying tumor cells may be transferred to living cells via the uptake of apoptotic bodies and may contribute to tumor progression. DNA encoding *H-ras*^{V12} and c-*myc* oncogenes may be transferred to the nucleus of the phagocyte but will only integrate and propagate in p53- and p21-deficient mouse embryonic fibroblasts, whereas normal cells are resistant to transformation. Here, we show that this protective mechanism (activation of p53 and p21 after uptake of apoptotic bodies) is dependent on DNA fragmentation, where inhibition of the caspase-activated DNase in the apoptotic cells, in conjunction with genetic ablation of lysosomal DNase II in the phagocytes, completely blocks p53 activation and consequently allows DNA replication of transferred DNA. We, therefore, suggest that there is a causal relationship between DNA degradation during apoptosis and p53 activation. In addition, we could further show that Chk2$^{-/-}$ cells were capable of replicating the *hyg*^{R} gene taken up from engulfed apoptotic cells, suggesting involvement of the DNA damage response. These data show that the phagocytosing cell is sensing the degraded DNA within the apoptotic cell, hence preventing these genes from being replicated, probably through activation of the DNA damage response. We, therefore, hypothesize that *DNase II* together with the *Chk2, p53,* and *p21* pathway form a genetic barrier blocking the replication of potentially harmful DNA introduced via apoptotic bodies, thereby preventing transformation and malignant development. (Mol Cancer Res 2006;4(3):187–95)

Introduction

The genomic integrity of an individual cell is threatened by DNA-damaging agents, such as UV or ionizing radiation, mutagenic chemicals, and endogenous oxygen radicals generated by normal metabolism. Another potential insult to the integrity of the genome is the horizontal transfer of genetic material from dead cells via the uptake of apoptotic bodies. We and others have shown that genetic information may be transferred from dying to living cells via the uptake of apoptotic bodies (1-3). However, transfer of apoptotic DNA to normal fibroblast or endothelial cells results in cell cycle arrest and senescence and is therefore not replicated to its daughter cells (2, 4). The p53 tumor suppressor is a central mediator of cellular responses to DNA damage and other forms of cellular stress (5, 6). Abnormalities of the *p53* tumor suppressor gene are thought to be central to the development of a high proportion of human tumors. We have previously shown that mouse embryonic fibroblasts (MEF) deficient in the *p53* gene or its transcriptional target *p21* differ from normal cells as they are able to replicate DNA taken up from apoptotic bodies (Table 1). Furthermore, apoptotic bodies derived from a *H-ras*^{V12}– and human c-*myc*–transformed rat fibrosarcoma were able to transform MEF p53- or p21-deficient cells but not wild-type MEF cells (4, 7). Integration and propagation of the tumor-derived *H-ras*^{V12} and human c-*myc* oncogenes could be verified by fluorescence *in situ* hybridization analysis of the resulting mouse tumor cells. These findings indicate that horizontal gene transfer between tumor cells may be a driving force of genomic instability and high mutability of tumor cells, and that the p53/p21 pathway protects normal cells against propagation of potentially harmful DNA (8).

To further investigate how cells are protected against incoming apoptotic DNA, we hypothesized that fragmented DNA from dead cells may activate the DNA damage response of the phagocyte. Here, we show for the first time that DNA degradation of apoptotic DNA by the caspase-activated DNase (CAD) and especially DNase II enzymes is necessary for activation of the DNA damage pathway within the phagocytosing cell. Furthermore, we provide evidence that activation of the Chk2/p53/p21 pathway by these DNA fragments blocks replication of genomic DNA that has been transferred from apoptotic cells. Chk2 is a critical regulator of p53 functions because cells derived from Chk2-deficient mice have a defective G_1-S checkpoint, apoptosis, and the transcriptional induction of p53 target genes, such as *p21*^{Waf1}, *Bax*, and *Noxa* (9, 10). Thus, Chk2 is a key component of a highly conserved DNA damage response signaling pathway, where p53 is one critical target. Here, we show that genetic ablation of either the *DNase II* or *Chk2* gene abolishes the activation of p53 and

Received 12/18/05; revised 1/27/06; accepted 2/1/06.
Grant support: Swedish Cancer Society, Swedish Society of Medicine, Cancerföreningen Stockholm, Lennander's Foundation, and Karolinska Institutet. The costs of publication of this article were defrayed in part by the payment of page charges. This article must therefore be hereby marked advertisement in accordance with 18 U.S.C. Section 1734 solely to indicate this fact.
Requests for reprints: Lars Holmgren, Cancer Center Karolinska Hospital, Karolinska Institutet, S-171 76 Stockholm, Sweden. E-mail: lars.holmgren@cck.ki.se

doi:10.1158/1541-7786.MCR-05-0262

Table 1. Results from Cocultivation of MEFs Together with Apoptotic Tumor Cells

Recipient cells	p53 induction	Hygromycin resistant	Focus formation	Tumor
Wild-type MEF	+	–	–	–
DNase II$^{-/-}$	–/+	+	–	ND
Chk2$^{-/-}$	–	+	–	–
p53$^{-/-}$	–	+	+	+
p21$^{-/-}$	+	+	+	+

NOTE: Coculture of apoptotic cells, containing the oncogenes c-*myc* and *H-ras*^{V12} together with the *hyg*^{R} gene, with MEFs will lead to different outcome depending on the genetic background of the cells. Our data indicate that p53, p21, Chk2, and DNase II protect the phagocytosing cells from propagation of incoming DNA.

allows replication of foreign genomic DNA. Therefore, we suggest that the DNase II enzyme together with the Chk2/p53/p21 DNA damage pathway form a protective barrier against horizontally transferred DNA. This genetic barrier may guard the genomic integrity of normal cells and thereby prevent transformation and malignant development.

Results

DNA Fragmentation in the Apoptotic Body Determines the Kinetics of p53 Induction in the Phagocyte

Induction of apoptosis will result in condensation of chromatin, and this is later followed by cleavage of the DNA. This DNA fragmentation requires activation of DNases; therefore, we analyzed the role of DNA fragmentation by inhibition of the responsible DNases. One of the DNases responsible for DNA degradation during apoptosis is CAD (11). CAD is normally forming a complex with ICAD, its inhibitor, that is cleaved by caspases during apoptosis, and CAD is thereby activated (12, 13). We transfected rat embryonic fibroblasts (REF) with the *H-ras*^{V12}, human c-*myc* oncogenes, and the *hyg*^{R} gene (REFrmh cells) to use as donor cells. To study the role of DNA degradation, these REFrmh cells were transfected with mutant ICAD (ICADLdm) that can not be cleaved by caspases, and DNA fragmentation in the apoptotic cell is thereby prevented (14). Analysis of DNA integrity by DNA fragmentation gels showed that ICADLdm expression efficiently inhibited ladder formation after apoptosis induced by nutrient depletion (Fig. 1A). To study the effect of CAD inhibition on p53 induction in the phagocytosing cell, apoptosis was induced by nutrient depletion in REFrmh or REFrmh-ICADLdm cells, and the resulting apoptotic cells were cocultured with MEF cells. The kinetics of p53 induction was analyzed by Western blot 4, 8, 12, and 24 hours after the initiation of the cocultivation, where the induction of p53 was shifted 4 hours and peaked 12 hours after the addition of the apoptotic REFrmh-ICADLdm cells (Fig. 1B and C).

Inhibition of DNA Fragmentation by CAD and DNase II Inhibits p53 Induction

The inhibition of CAD in the donor cell delayed but did not completely inhibit p53 induction. We therefore investigated the involvement of DNases localized in the lysosomes of the phagocytes. For this purpose, we used Bafilomycin A1, a specific irreversible inhibitor of vacuolar H^+/ATPase, resulting in inhibition of acidification in endosomes and in lysosomes

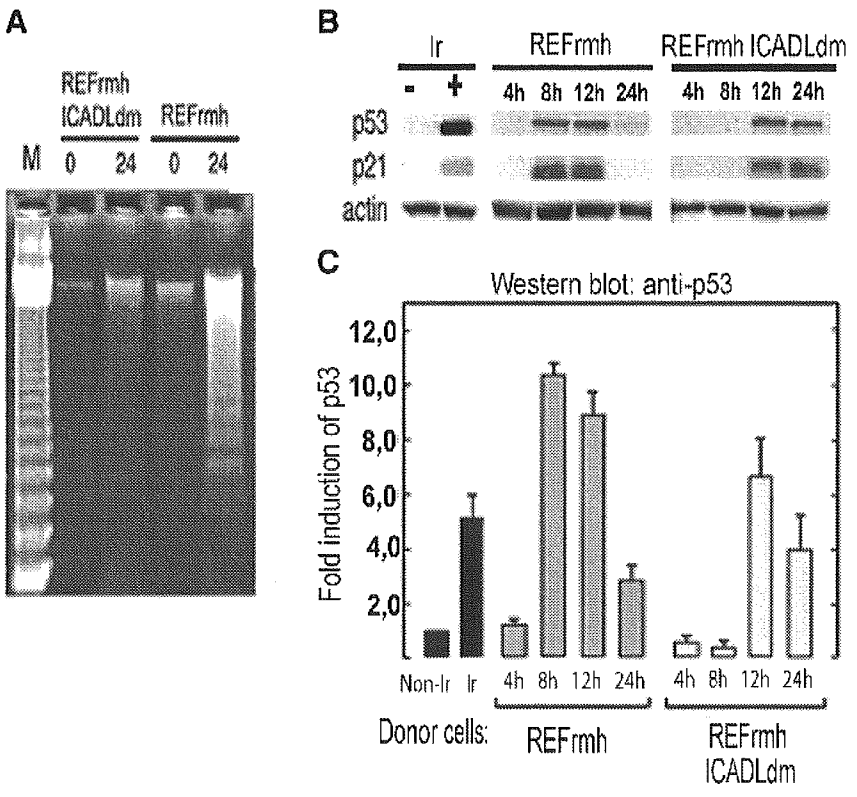

FIGURE 1. Inhibition of DNA fragmentation in the dying cells shifts the kinetics of p53 activation. **A.** Donor REFrmh cells were retrofected with ICAD-Ldm or empty vector. Positive cells were selected with puromycin. Five millions cells were harvested, and the nuclei were pelleted by centrifugation. Fragmentation of DNA in the supernatant was analyzed by agarose gel electrophoresis. The cells were either cultured in growth medium or exposed to nutrient depletion for 24 hours. A 123-bp ladder was used as a reference (*M*). Nutrient depletion induced DNA fragmentation in the vector-transfected REFrm cells, whereas expression of ICAD-Ldm efficiently inhibited DNA fragmentation. **B.** Western blot analysis of the kinetics of p53 and p21 induction after feeding MEF cells with either REFrm or REFrm-ICADLdm apoptotic bodies. **C.** Levels of p53 accumulation in three independent experiments. Bars, SD.

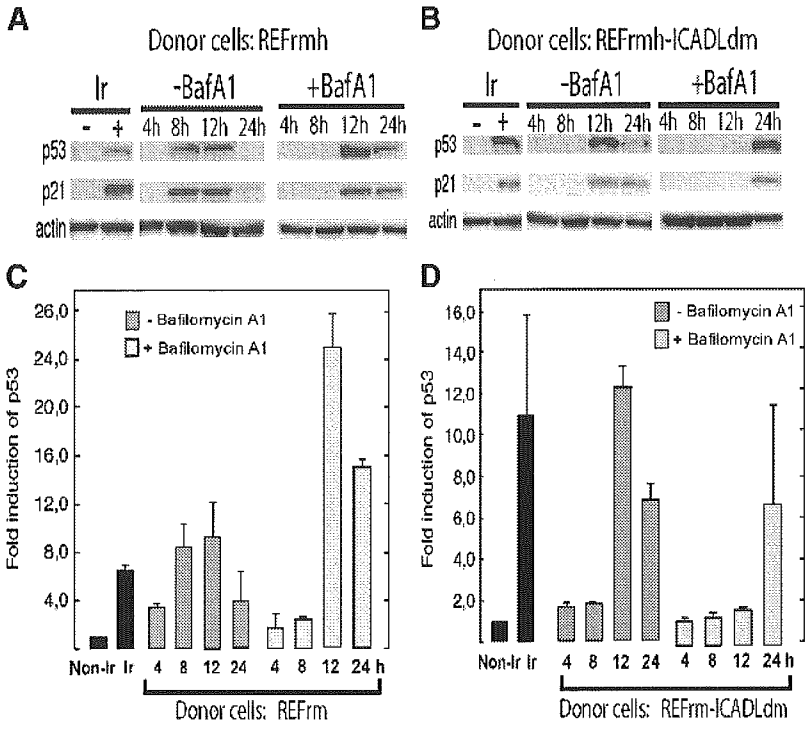

FIGURE 2. Inhibition of lysosomal DNA fragmentation delays the induction of p53. DNA fragmentation in the lysosomal was inhibited by treating the recipient cells with Bafilomycin A1 as previously reported by McIlroy et al. (14). **A.** Western blot analysis of p53 and p21 induction after addition of apoptotic bodies. Cells (*right*) were treated as described in Materials and Methods with Bafilomycin A1. **B.** Effect of inhibiting both CAD and lysosomal DNase activity on p53 induction using REFrmh-ICADLdm donor cells together with Bafilomycin A1. **C.** Levels of p53 accumulation in three independent experiments. **D.** Levels of p53 accumulation in three independent experiments. Bars, SD.

and thus indirect inhibition of lyzosomal DNase activity (15). Recipient MEFs were treated with Bafilomycin A1 during the cultivation with apoptotic cells. Inhibition of lysosomal acidification resulted in shifted kinetics of p53 accumulation, which peaked at 12 hours (Fig. 2A and C). To test the effect of combination of inhibiting the CAD and DNase II, we used REFrm-ICADLdm as donors together with Bafilomycin A1. The joint inhibition of CAD in the dying cell and lysosomal acidification in the phagocytosing cell resulted in a further delay in p53 accumulation, which now peaked at 24 hours (Fig. 2B and D).

DNase II has previously been shown to be essential for degradation of apoptotic DNA in the lysosomes of the phagocytosing cell (16); therefore, we tested the effect of

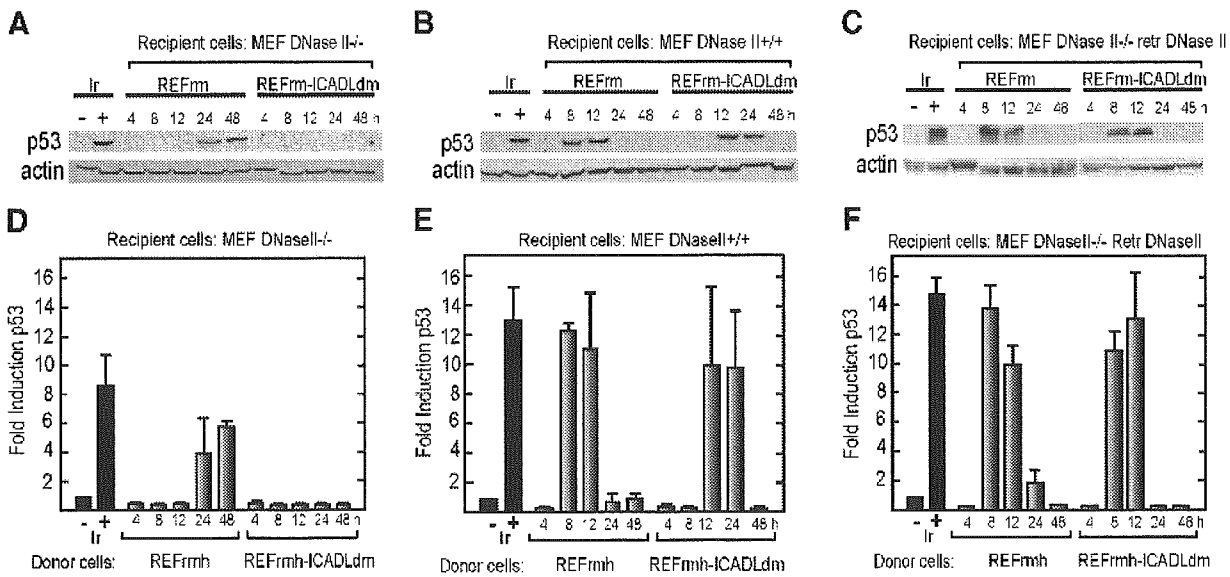

FIGURE 3. Inhibition of CAD and lysosomal DNase II completely blocks p53 activation induced by apoptotic bodies. **A.** Western blot analysis of p53 activation in DNase II–deficient MEF cells after addition of either REFrmh or REFrmh-ICADLdm. **B.** Western blot analysis of p53 activation in wild-type MEF cells after addition of either REFrmh or REFrmh-ICADLdm. **C.** Western blot analysis of p53 induction in DNase II–deficient MEF cells retransfected with DNase II, after addition of either REFrmh or REFrmh-ICADLdm apoptotic cells. **D.** Levels of p53 accumulation in DNase $II^{-/-}$ MEF cells in three independent experiments. **E.** Levels of p53 accumulation in wild-type MEF cells in three independent experiments. **F.** Levels of p53 accumulation in MEF DNase $II^{-/-}$ cells retransfected with DNase II in three independent experiments. Bars, SD.

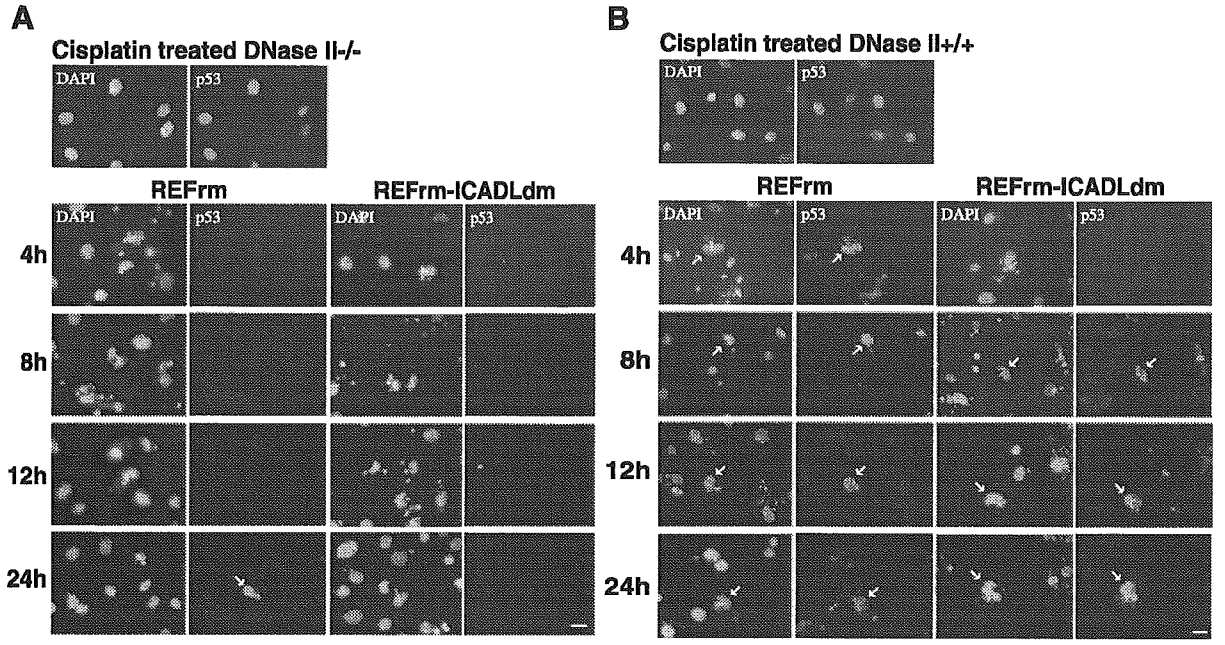

FIGURE 4. Induction of p53 in the phagocyte is dependent on DNA fragmentation in the apoptotic body. **A.** Wild-type MEF cells. Top, positive control of p53 staining of cells treated with cisplatin for 4 hours. Bottom, induction of p53 in cells at indicated time points after incubation with apoptotic REFrm or REFrm-ICADLdm. **B.** MEF DNaseII$^{-/-}$ cells. Top, positive control of p53 staining in cells treated with cisplatin for 4 hours. Bottom, induction of p53 in cells at indicated time points after incubation with apoptotic REFrm or REFrm-ICADLdm. Arrows, positive nuclei. Bar, 10 μm.

genetic ablation of DNase II on p53 activation. MEF cells lacking DNase II activity resulted in a dramatic shift in p53 induction, which occurred at 24 hours compared with DNaseII$^{+/+}$ cells, where p53 was induced at 8 hours (Fig. 3A, B, D, and E). As a control, DNase II enzyme was retransfected into DNaseII$^{-/-}$ cells, and in these cells, the p53 kinetics was restored (Fig. 3C and F). Immunostaining showed an even more dramatic shift in p53 induction, where p53 induction was detected already at 4 hours in DNaseII$^{+/+}$ cells compared with 24 hours in DNaseII$^{-/-}$ cells (Fig. 4A and B). Furthermore, no p53 induction could be detected by Western blot analysis when both CAD and DNase II enzyme activities were blocked (Fig. 3A and D). These data were confirmed by immunostaining, where no p53 induction could be detected within the DNase II$^{-/-}$ phagocytes after addition of apoptotic cells lacking functional CAD (Fig. 4A).

Horizontally Transferred DNA Is Replicated in Cells with Inactive DNase II

The lack of p53 induction argued that DNase II–deficient cells may be permissive for replicating genomic DNA transferred from engulfed dying cells.

Apoptotic REFrm, REFrmh, or REFrmh-ICADLdm was added to DNase II$^{-/-}$ cells, and resistant colonies were selected with hygromycin. Cocultivation of DNase II$^{-/-}$ cells with either the REFrmh or REFrmh-ICADLdm resulted in stable propagation of the *hyg*^{R} gene and the growth of hygromycin-resistant colonies, although at different frequencies (Fig. 5A; Table 1). Retransfection of the *DNase II* gene completely blocked the formation of hygromycin-resistant colonies (Fig. 5B), and p53 induction was detected 8 hours after coculture with apoptotic REFrmh cells (Fig. 3C and F). This emphasize that DNase II plays an essential role in protecting cells from replicating genomic DNA acquired from dying cells.

Transfer of DNA into Chk2$^{-/-}$ Cells

Our data suggest that DNA degradation in the apoptotic cell in some way activates p53, and that this plays an important role in protecting the phagocytosing cell from replicating horizontally transferred DNA. It is, therefore, plausible to believe that the degraded apoptotic DNA is sensed by the DNA damage response of the phagocytosing cell, resulting in the induction of p53. Chk2 has been implicated as a mediator of p53 activation triggered by DNA damage; therefore, we assessed the role of Chk2 in the cellular response to fragmented DNA from apoptotic cells. For this purpose, we tested whether the hygromycin resistance gene (*hyg*^{R}) could be transferred to Chk2$^{-/-}$ MEF cells.

Apoptotic REFrmh cells were cocultured with MEF Chk2$^{+/+}$ or MEF Chk2$^{-/-}$ cells. Apoptotic REFrm cells lacking the *hyg*^{R} gene (REFrm) were used as a negative control, and recipient MEF p21$^{-/-}$ cells served as a positive control. Selection for hygromycin-resistant cells was started 48 hours after the apoptotic bodies were added to the recipient cells. Resistant colonies, visualized by Coomassie staining, were detected 14 to 16 days later in plates where REFrmh apoptotic bodies had been cocultured with MEF Chk2$^{-/-}$ cells (Fig. 6A; Table 1). No colonies were detected in MEF Chk2$^{+/+}$ cells cocultured with REFrmh cells or in MEF Chk2$^{-/-}$ cells fed with apoptotic bodies lacking the *hyg*^{R} gene. The frequency of colony formation was counted in triplicates as shown in Fig. 6B, where ~1 of 10,000 MEF Chk2$^{-/-}$ cells had generated resistance to hygromycin treatment.

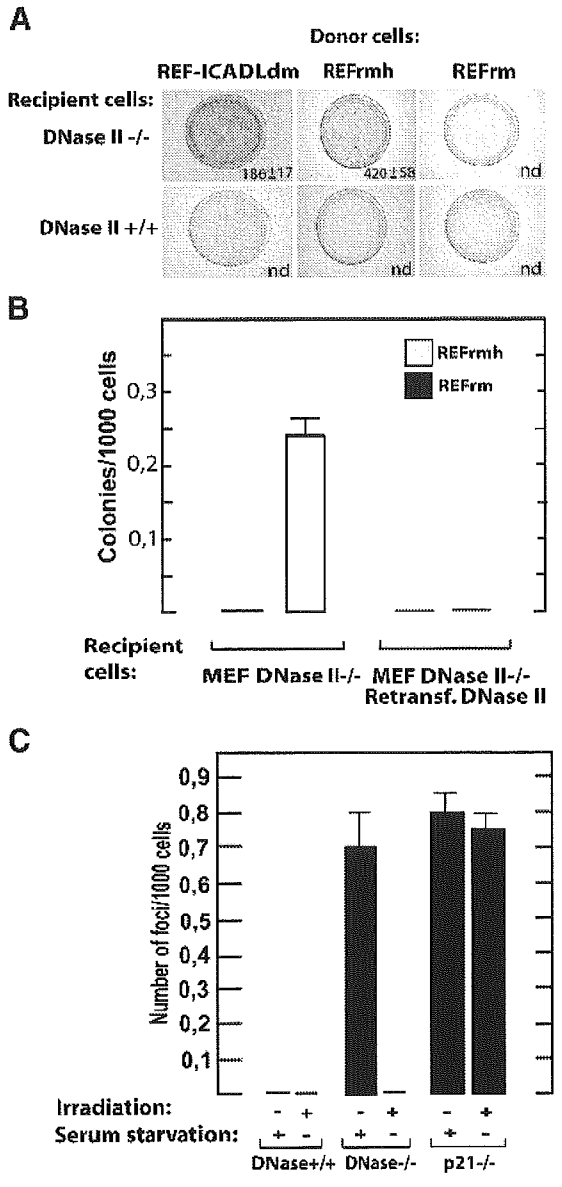

FIGURE 5. Genetic inactivation of DNase II allows stable replication of genes transferred from apoptotic bodies. **A.** DNase $II^{-/-}$ and DNase $II^{+/+}$ cells, respectively, were cocultivated with REFrmh or REFRmh-ICADLdm apoptotic bodies, and resistant colonies were selected for with hygromycin as described in Materials and Methods. REFrm cells lacking the hyg^R gene served as a negative control. Columns, number of colonies per 10-cm Petri dish from triplicates; bars, SD. nd, non-detectable. **B.** DNase $II^{-/-}$ cells retrofected with the mouse *DNase II* gene were incubated with apoptotic bodies derived from REFrm or REFrmh cells. Colonies per 1,000 cells after 2 weeks of hygromycin selection. **C.** DNA degradation by CAD does not inhibit propagation of transferred DNA. Wild type, DNase $II^{-/-}$, or $p21^{-/-}$ cells were cocultivated with REFrmh apoptotic cells, and resistant colonies were selected for with hygromycin as described in Materials and Methods. Apoptosis in the donor cells was induced by nutrient depletion. As indicated, apoptosis was induced by γ-irradiation (150 Gy) in some of the donor cells to induce double-strand breaks. Colonies per 1,000 cells after 2 weeks of hygromycin selection. No hygromycin-resistant colonies were observed, where wild-type MEF cells were used as recipient cells. Interestingly, DNase $II^{-/-}$ MEFs acquired the hyg^R gene from REFrm apoptotic bodies killed by nutrient depletion, but induction of double-strand breaks by irradiation totally blocked propagation of transferred DNA. In contrast, $p21^{-/-}$ cells were able to acquire the hyg^R gene independent on whether the donor cells had been irradiated or not.

The mouse origin of the colonies was verified by mouse-specific MHC staining (data not shown). Colonies from MEF $Chk2^{-/-}$ cells cocultured with REFrmh cells were harvested, and DNA was isolated from these cells. The presence of the hygromycin resistance gene in these cells was shown by PCR analysis (Fig. 6B). In addition, transfer of $H\text{-}ras^{V12}$ and human c-*myc* could also be detected by PCR. These data show that Chk2-deficient cells are capable of propagating DNA from apoptotic bodies.

MEFs deficient for either the *p53* or *p21* genes are transformed by the uptake of apoptotic REFrmh cells *in vitro* and form tumors when injected into severe combined immunodeficient mice (4, 7). Because we could detect transfer of the c-*myc* and $H\text{-}ras^{V12}$ oncogenes to the $Chk2^{-/-}$ cells by PCR, we tested whether this resulted in a tumorigenic phenotype. MEF $Chk2^{-/-}$ cells were cultured with apoptotic REFrm cells or nontransformed REF cells for 10 days before injection into severe combined immunodeficient mice. Twelve of 15 animals of the positive control, MEF $p21^{-/-}$ cells cocultured with apoptotic REFrm cells, formed tumors within 1 week and were euthanized due to tumor size within 30 days after injection. In contrast, no tumor development was detected in any of the mice injected with MEF $Chk2^{-/-}$ cells cocultured with apoptotic REFrmh cells (Fig. 6E; Table 1). These results show that Chk2-deficient cells are able to salvage and replicate DNA from apoptotic bodies but are not transformed by the transferred $H\text{-}ras^{V12}$ and c-*myc* oncogenes.

Apoptotic Bodies Induce Chk2-Dependent Accumulation of p53 and p21 Proteins

Following its activation, Chk2 phosphorylates not only p53 but a set of effector molecules, including Brca1, E2F, pml, and Plk3, that are involved in checkpoint control (17). However, our previous data clearly indicate an essential role of the p53/p21 pathway in controlling replication of apoptotic DNA. We, therefore, assessed whether p53 is activated by the addition of apoptotic bodies and whether this induction was Chk2 dependent. Addition of apoptotic bodies to wild-type MEF cells resulted in rapid engulfment (Fig. 6C) and induction of p53 protein 8 hours later in the phagocytosing cells (Fig. 7A and D). Induction of the *p21* target gene was also detected with similar kinetics. In contrast, coculture of MEF $Chk2^{-/-}$ with apoptotic bodies did not yield any detectable accumulation of p53 or p21 (Fig. 7B and D), although the frequency of phagocytosed dead cells did not differ. The p53/p21 pathway was intact in the Chk2-deficient cells, as both proteins could be induced after UV irradiation. Furthermore, the increased p53 and p21 protein levels were not derived from the engulfed apoptotic donor cells, as no positive signal could be detected in the apoptotic cells when cultured alone (Fig. 7C).

Immunofluorescence staining confirmed the data from the Western blot analysis, showing that cells containing apoptotic bodies were p53 positive (Fig. 7E). The positive staining was only localized in the nuclei of the phagocytosing cells, as no staining was detected in the ingested apoptotic bodies. As expected from the Western blot results, the $Chk2^{-/-}$ recipient cells that had engulfed apoptotic bodies remained p53 negative, as indicated by arrows. In conclusion, engulfment of apoptotic cells trigger Chk2-dependent p53 accumulation and p21 activation in the phagocytosing cell.

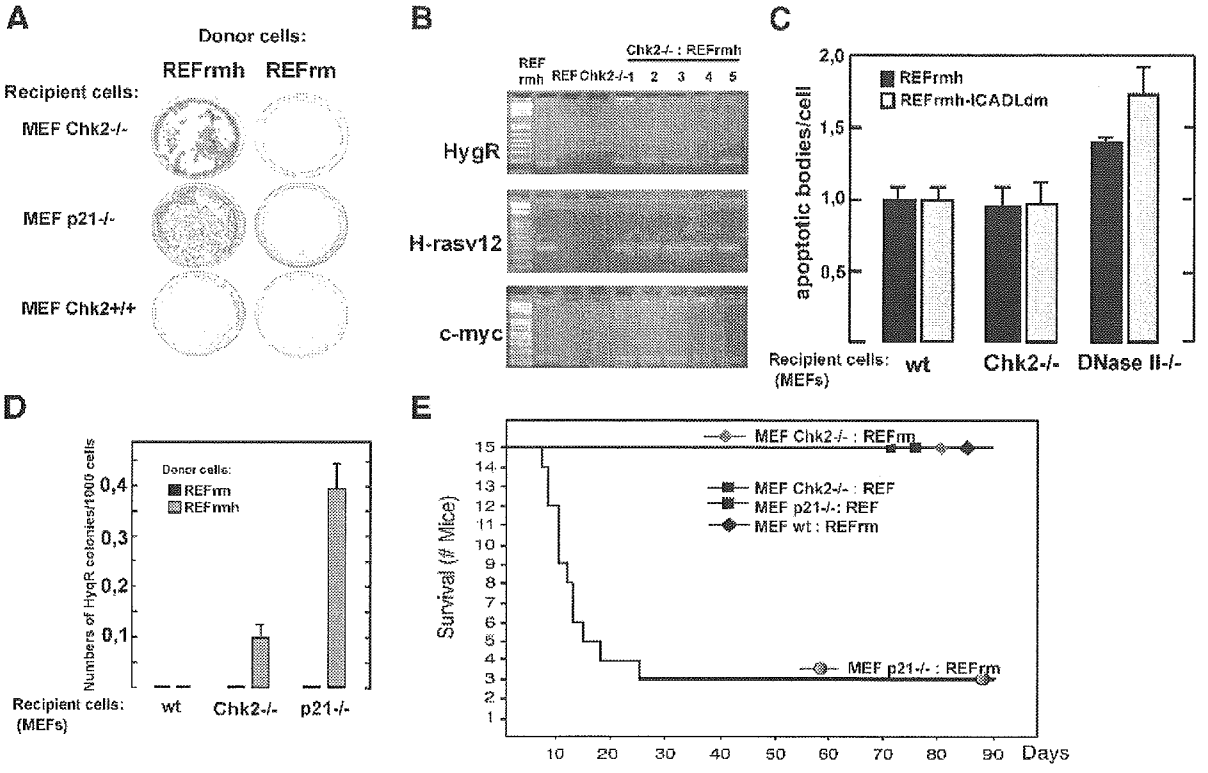

FIGURE 6. The hyg^R gene is stably transferred to and propagated by MEF Chk2$^{-/-}$ cells after coculture with apoptotic REFrmh cells. **A.** MEF Chk2$^{-/-}$ cells cocultured with apoptotic REFrmh cells result in colony formation after selection with hygromycin. Apoptotic REFrm cells lacking the hyg^R gene serve as negative control. Coomassie staining shows colony formation in MEF Chk2$^{-/-}$ cells but not in the MEF Chk2$^{+/+}$ cells cocultured with REFrmh. No colonies were detected where MEF Chk2$^{+/+}$ or MEF Chk2$^{-/-}$ cells were cocultured with REFrm cells lacking the hyg^R gene. MEF p21$^{-/-}$ cells were used as positive control. **B.** PCR analysis of the presence of the hyg^R, *c-myc*, and *H-ras*^{V12} genes in the MEF Chk2$^{-/-}$ colonies that developed after coculture with REFrmh cells and selection with hygromycin. **C.** Analysis of phagocytotic activity of wild type (*wt*), Chk2$^{-/-}$, and DNase II$^{-/-}$ MEFs. Apoptotic bodies from REFrm or REFrm-ICADLdm cells killed by nutrient deprivation were added to the indicated MEFs and incubated for 2 hours. The number of ingested apoptotic bodies per engulfing cells was analyzed and quantified by counting total number of ingested bodies per total number of cells. **D.** Frequency of colony formation in MEF Chk2$^{-/-}$ cells cocultured with apoptotic REFrmh cells. No colony formation was detected in MEF Chk2$^{+/+}$ cells. Columns, average from three independent experiments; bars, SD. **E.** MEF Chk2$^{-/-}$ cells cocultured with REFrm apoptotic cells were not tumorigenic. MEF Chk2$^{+/+}$, MEF Chk2$^{-/-}$, and p21$^{-/-}$ cells cocultured with apoptotic REFrmh or REF cells were injected in the dorsal s.c. space of severe combined immunodeficient mice. Twelve of 15 mice injected with MEF p21$^{-/-}$ cells cocultured with REFrm cells developed tumors. No tumor development was detected in mice injected with MEF Chk2$^{+/+}$, MEF Chk2$^{-/-}$, and p21$^{-/-}$ cells cocultured with REF cells *in vitro*. From two independent experiments.

Discussion

The role of apoptosis in healthy individuals is to eliminate unwanted and potentially harmful cells. These apoptotic cells are rapidly cleared by macrophages or neighboring cells *in vivo* (18). We have previously shown that DNA from dying cells is transferred to living cells via the uptake of apoptotic bodies and may contribute to tumor progression. Here, we provide evidence that the apoptotic DNA degraded in the lysosomes by DNase II activates the DNA damage response of the phagocytosing cells and thus prevents propagation of potentially pathologic DNA acquired by engulfment of apoptotic cells.

In this study, we found that DNase II plays an essential role in the activation of p53 and the consequent inhibition of replicating transferred DNA. DNase II has been shown to be responsible for degradation of DNA from apoptotic bodies in macrophages where genetic inactivation of DNase II inhibits DNA degradation of engulfed dead cells, as shown by terminal deoxynucleotidyl transferase–mediated nick end labeling staining, resulting in accumulation of apoptotic bodies in the cytoplasm of macrophages (14). Furthermore, DNase II acts as a lysosomal barrier to transfection with nonviral expression vectors (19). This effect was specific for transfection methods that introduce DNA into cells by endocytosis but not other methods (e.g., electroporation). Our data indicate that the lysosomal degradation of DNA from the engulfed apoptotic cell is critical for the activation of p53 in the phagocytosing cell. Furthermore, joint inhibition of CAD and DNase II totally blocked p53 activation. These data argue in favor for the hypothesis that apoptotic DNA, similar to transfected DNA, may enter the nucleus via the endosomal/lysosomal pathway. We propose that the DNase II–cleaved DNA from engulfed apoptotic cells triggers a DNA damage response in the nucleus of the phagocyte (Fig. 8). We have indeed shown local colocalization of the DNA damage markers MRE11 and gamma H2AX with apoptotic DNA labeled with bromodeoxyuridine in the nucleus of the recipient cell.[4]

The inhibition of the DNA degradation blocked induction of p53, and consequently, DNA transferred from apoptotic cells (hyg^R gene) could be replicated. Retransfection of the

[4] J. Ehnfors, unpublished data.

DNase II gene into the DNase $II^{-/-}$ cells restored the protection against replication of salvaged DNA, and no hyg^R colonies could be detected (Fig. 5B). In these retransfected cells, accumulation of p53 could be detected with a similar kinetics as wild-type MEF cells after coculture with apoptotic cells (Fig. 3C and F). It is also interesting to note that DNA was transferred to DNase $II^{-/-}$ recipient cells even when cocultured with apoptotic bodies with DNA degraded by CAD activity, whereas induction of double strand breaks using γ-irradiation completely blocked DNA transfer (Fig. 5A and C). A possible explanation to these apparently contradictory data is that the qualitative difference of the generated DNA fragments may affect the cellular response. CAD cleaves DNA generating, blunt-ended, double-stranded fragments carrying 5′-phosphate and 3′-hydroxyl groups, whereas lysosomal degradation mediated by DNase II generates 5′-hydroxyl and 3′-phosphate ends (20, 21). An alternative explanation could be that DNA cleaved by CAD in the serum-starved donor cells triggers a weaker/later p53 response in the DNase $II^{-/-}$ recipient cells compared with DNA with double-strand breaks in the γ-irradiated donor cells. A delayed or weak p53 response could result in recipient cells becoming more susceptible to horizontally transferred DNA.

We have previously shown that normal cells are able to take up DNA from apoptotic bodies but are subsequently cell cycle arrested, thus preventing DNA replication. Here, we show that uptake of apoptotic cells results in p53 induction of the phagocytosing cell, and that this is not only due to functional DNases but also to functional Chk2, as no detectable accumulation of p53 or p21 could be detected in Chk2-deficient cells. MEF cells lacking the *Chk2* gene have lost the cell cycle checkpoint, as these cells could acquire and replicate the hyg^R gene from apoptotic cells (Table 1). Interestingly, we could also detect transfer of the $H\text{-}ras^{V12}$ and c-*myc* oncogenes that, however, did not result in a transformed or a tumorigenic phenotype, as the hygromycin-resistant colonies became senescent when propagated *in vitro* (data not shown). This is in contrast to $p53^{-/-}$ or $p21^{-/-}$ recipient cells that readily form tumors after uptake of oncogenic DNA (Table 1). These

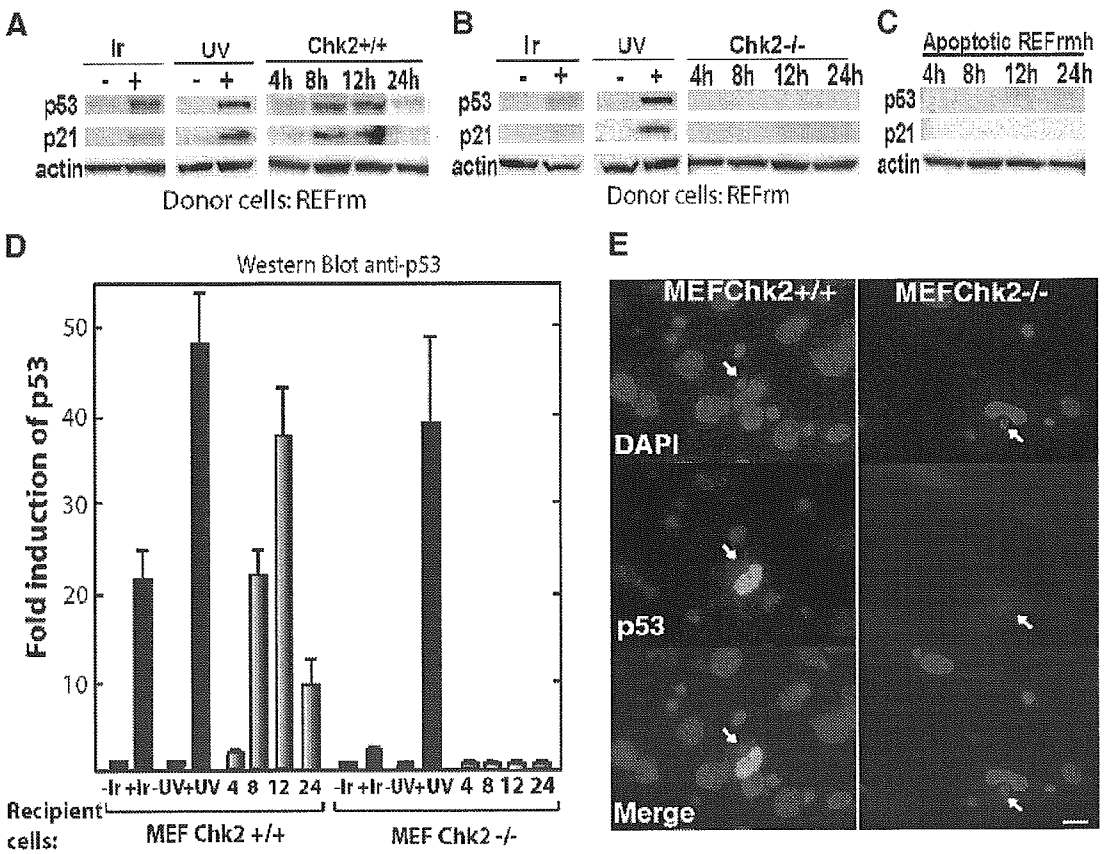

FIGURE 7. Uptake of apoptotic bodies induces Chk2-dependent activation of p53. Apoptosis was induced in REFrm cells by nutrient depletion and added to MEF $Chk2^{+/+}$ or $Chk2^{-/-}$ cells. Induction of p53/p21 by γ or UV irradiation served as positive controls. **A.** Induction of p53 and p21 was analyzed by Western blot in $Chk2^{+/+}$ MEF cells after cultivation with apoptotic REFrm cells for 4, 8, 12, and 24 hours. Induction of both p53 and p21 was detected after 8 hours. **B.** In contrast, although UV irradiation triggered a readily detectable p53 response, addition of apoptotic bodies did not induce p53 or p21 in MEF $Chk2^{-/-}$ cells. **C.** No positive signal could be detected in lysates from apoptotic bodies cultured alone during the same incubation times. **D.** Quantification of p53 accumulation in three independent experiments. Bars, SD. **E.** Chk2-dependent accumulation of p53 in the nuclei of cells phagocytosing apoptotic bodies. Top, 4′,6-diamidino-2-phenylindole (*DAPI*) staining of cells cultured with apoptotic bodies. Middle, total p53 staining. Bottom, composite of 4′,6-diamidino-2-phenylindole + p53 stainings. Note that the apoptotic bodies stain negative for p53, whereas the recipient MEF $Chk^{+/+}$ cells are positive. p53 staining was not detectable in $Chk2^{-/-}$ cells. Arrows, engulfed apoptotic bodies. Bar, 10 μm.

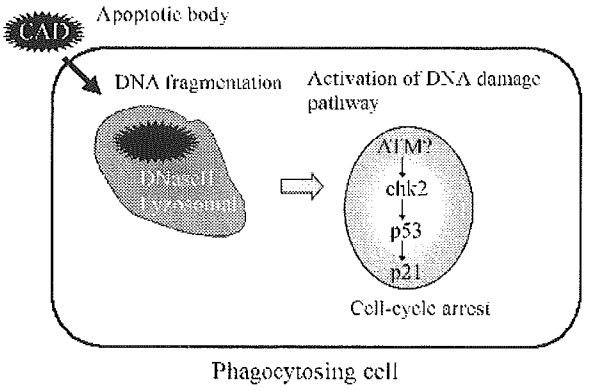

FIGURE 8. Schematic figure of our hypothesis. We suggest that the Chk2/p53/p21 DNA damage pathway in the phagocytosing cell, together with the DNase II enzyme, form a genetic barrier against horizontally transferred DNA, blocking replication of foreign DNA from engulfed apoptotic cells. This genetic barrier may guard the genomic integrity of normal cells.

findings indicated that Chk2 may primarily respond to the incoming DNA but is not protecting against tumor transformation. Because the Chk2-deficient cells contain an intact $p19^{ARF}$ gene, it is likely that the transferred oncogenes activate p53 via the $p19^{ARF}$ pathway and thus prevents transformation.

During its lifetime, the somatic cell is exposed to genotoxic stress, such as alkylating agents, oxygen radicals, and ionizing radiation. To this list of genomic insults, we would like to add DNA transfer from apoptotic bodies. The uptake of DNA may be a mere consequence of inadequate DNA degradation in the lysosomes, which is then transported into the nucleus. This may pose a serious threat to the integrity of the genome and may result in neoplastic transformation. We speculate that one role of the molecular pathway, starting with lysosomal DNA degradation leading to the Chk2-dependent p53 activation, is to protect the individual cell from propagating DNA taken up from apoptotic cells (Fig. 8). Malfunction of the checkpoint control may cause accumulation of genetic alterations, ultimately leading to cancer.

Materials and Methods

Cell Lines

REFs and MEFs from DNase $II^{-/-}$ $p21^{-/-}$, $Chk2^{-/-}$, and $Chk2^{+/+}$ mice were grown in DMEM with glutamin, penicillin/streptomycin, and 10% fetal bovine serum (4, 10, 21). REFrmh cells containing the *H-ras*^{V12}, human c-*myc*, and the hyg^R gene have been described (4). The REFrmh-ICADLdm (12) and transfection of DNase II into MEF DNase $II^{-/-}$ cells were generated as previously described (22), selected in puromycin (5 and 1 μg/mL, respectively; Sigma-Aldrich, St. Louis, MO).

Gene Transfer Experiments

Recipient MEFs (1×10^6) of indicated genetic backgrounds were plated in 10-cm Petri dishes. Apoptosis was induced in REFrmh cells by nutrient depletion, previously described (4), and verified by Hoechst 33258 and Annexin V staining. Five million apoptotic cells were added to each 10-cm Petri dish containing the MEF recipients. Forty-eight hours after addition of the apoptotic donor cells, the tissue culture medium was changed. Cells were grown in the presence of hygromycin (200 μg/mL; Sigma-Aldrich) to select for the uptake of the hyg^R gene in MEF cells. The resulting colonies were visualized by Coomassie staining.

PCR Analysis

DNA from hygromycin-resistant colonies was isolated with Qiaamp Blood kit (Qiagen, Chatsworth, CA). PCR analysis was done with specific primers and conditions for the human c-*myc*, the H-ras^{V12}, and the hyg^R genes as previously described (4).

Tumor Growth

MEF $Chk2^{+/+}$, MEF $Chk2^{-/-}$, or MEF $p21^{-/-}$ cells (1×10^6) cocultured with apoptotic REFrmh cells *in vitro* for 10 days, as indicated in the figure legends, were injected in the dorsal s.c. space of 6- to 8-week-old severe combined immunodeficient mice. Tumor growth was examined by palpation. Animals that did not develop tumors within 3 months were scored as negative.

Western Blot

For analysis of p53 induction by Western blot, cells were harvested [100 mmol/L Tris (pH 8), 150 mmol/L NaCl, 1% NP40, protease inhibitors cocktail] at 4, 8, 12, and 24 hours after the addition of apoptotic bodies. Protein concentration was measured (A_{595}, Bradford method), and samples were loaded (12% polyacrylamide gel, Bio-Rad, Richmond, CA). Transfer to Protean filter (Schleicher and Schuell, Keene, NH). Block with 5% milk for 1 hour at room temperature before incubation with primary antibody (anti-p53 FL-393, 1:400, Santa Cruz Biotechnology, Inc., Santa Cruz, CA and anti-p21, 1:200, BD PharMingen, San Diego, CA) overnight at 4°C or anti-β-actin (Sigma-Aldrich; 1:3,000) at room temperature for 1 hour, secondary antibody (anti-mouse-horseradish peroxidase or anti-rabbit-horseradish peroxidase NA 931 and NA 934V, 1:5,000; Amersham Pharmacia Life Science, Piscataway, NJ) for 2 hours at room temperature. The membrane was developed using detection system according to protocol of the manufacturer (Santa Cruz Biotechnology). MEF $Chk2^{+/+}$ cells (1×10^6) were plated on 10-cm Petri dishes; 50 nmol/L of Bafilomycin A1 (Sigma-Aldrich) was added 2 hours before addition of the apoptotic REFrmh and REFrmh-Ldm cells. Cells were then cocultured with or without Bafilomycin A1 and analyzed by Western blot at 4, 8, 12, and 24 hours as described above.

Fragmentation Assay

Apoptosis was induced (nutrient depletion) for 24 hours in 5×10^6 REFrmh cells with or without ICAD-Ldm. DNA fragmentation was analyzed as described (2).

Immunofluorescence

MEF $Chk2^{+/+}$ and MEF $Chk2^{-/-}$ cells were plated in chamber slides (Falcon, Lincoln, NJ) to adhere overnight. Nutrient depleted apoptotic cells were added and incubated for 4, 8, 16, and 24 hours, respectively. For total p53 staining, cells were fixed in methanol/acetone (1:1) for 10 minutes blocked with 5% horse serum and stained with primary antibody (anti-p53 FL-393, 1:100; Santa Cruz Biotechnology). Incubation for

30 minutes at room temperature with anti-rabbit FITC-conjugated secondary antibody (DAKO, Carpinteria, CA; 1:40), following mounting media containing 4′,6-diamidino-2-phenylindole (Vector Laboratories, Burlingame, CA).

References

1. de la Taille A, Chen MW, Burchardt M, Chopin DK, Buttyan R. Apoptotic conversion: evidence for exchange of genetic information between prostate cancer cells mediated by apoptosis. Cancer Res 1999;59:5461–3.

2. Holmgren L, Szeles A, Rajnavölgyi E, et al. Horizontal transfer of DNA by the uptake of apoptotic bodies. Blood 1999;93:3956–63.

3. Spetz AL, Patterson BK, Lore K, Andersson J, Holmgren L. Functional gene transfer of HIV DNA by an HIV receptor-independent mechanism. J Immunol 1999;163:736–42.

4. Bergsmedh A, Szeles, A, Henriksson M, et al. Horizontal transfer of oncogenes by uptake of apoptotic bodies. Proc Natl Acad Sci U S A 2001;98: 6407–11.

5. Lane DP. Cancer. p53, guardian of the genome. Nature 1992;358:15–6.

6. Levine AJ. p53, the cellular gatekeeper for growth and division. Cell 1997;88: 323–31.

7. Bergsmedh A, Szeles A, Spetz AL, Holmgren L. Loss of the p21(Cip1/Waf1) cyclin kinase inhibitor results in propagation of horizontally transferred DNA. Cancer Res 2002;62:575–9.

8. Holmgren L, Bergsmedh A, Spetz AL. Horizontal transfer of DNA by the uptake of apoptotic bodies. Vox Sang 2002;83 Suppl 1:305–6.

9. Hirao A, Cheung A, Duncan G, et al. Chk2 is a tumor suppressor that regulates apoptosis in both an ataxia telangiectasia mutated (ATM)-dependent and an ATM-independent manner. Mol Cell Biol 2002;22:6521–32.

10. Takai H, Naka K, Okada Y, et al. Chk2-deficient mice exhibit radio-resistance and defective p53-mediated transcription. EMBO J 2002;21: 5195–205.

11. Enari M, Sakahira H, Yokohama H, Okawa K, Iwamatsu A, Nagata S. A caspase-activated DNase that degrades DNA during apoptosis, and its inhibitor ICAD. Nature 1998;391:43–50.

12. Sakahira H, Enari M, Nagata S. Cleavage of CAD inhibitor in CAD activation and DNA degradation during apoptosis. Nature 1998;391:96–9.

13. Sakahira H, Takemura Y, Nagata S. Enzymatic active site of caspase-activated DNase (CAD) and its inhibition by inhibitor of CAD. Arch Biochem Biophys 2001;388:91–9.

14. McIlroy D, Tanaka M, Sakahira H, et al. An auxiliary mode of apoptotic DNA fragmentation provided by phagocytes. Genes Dev 2000;14:549–58.

15. Bowman EJ, Siebers A, Altendorf K. Bafilomycins: a class of inhibitors of membrane ATPases from microorganisms, animal cells, and plant cells. Proc Natl Acad Sci U S A 1988;85:7972–6.

16. Nagata S, Nagase H, Kawane K, Mukae N, Fukuyama H. Degradation of chromosomal DNA during apoptosis. Cell Death Differ 2003;10:108–16.

17. Motoyama N, Naka K. DNA damage tumor suppressor genes and genomic instability. Curr Opin Genet Dev 2004;14:11–6.

18. Savill J, Fadok V. Corpse clearance defines the meaning of cell death. Nature 2000;407:784–8.

19. Howell DP, Krieser RJ, Eastman H, Barry A. Deoxyribonuclease II is a lysosomal barrier to transfection. Mol Ther 2003;8:957–63.

20. Rosl F. A simple and rapid method for detection of apoptosis in human cells. Nucleic Acids Res 1992;20:5243.

21. Kawane K, Fukuyama H, Kondoh G, et al. Requirement of DNase II for definitive erythropoiesis in the mouse fetal liver. Science 2001;292:1546–9.

22. Troyanovsky B, Levchenko T, Mansson G, Matvijenko O, Holmgren L. Angiomotin: an angiostatin binding protein that regulates endothelial cell migration and tube formation. J Cell Biol 2001;152:1247–54.

J Bone Miner Metab (2004) 22:399–403
DOI 10.1007/s00774-004-0517-z

Journal of
Bone and
Mineral
Metabolism

Mini review

Progeroid syndrome as a model for impaired bone formation in senile osteoporosis

Akinori Hishiya* and Ken Watanabe

Department of Bone and Joint Disease, Research Institute, National Center for Geriatrics and Gerontology (NCGG), 36-3 Gengo, Morioka-cho, Obu 474-8522, Japan

Abstract Senile or age-related/dependent osteoporosis is caused by reduced bone formation, rather than increased bone resorption as in postmenopausal osteoporosis. Here we review genetically engineered mouse models with defects in osteoblastic proliferation or differentiation with focus on IGF signaling and stem cells. Model mice for human progeroid syndromes may provide useful tools for studying the pathogenesis of senile osteoporosis.

Key words premature aging syndrome · knockout mouse · osteoblast · differentiation · IGF

Introduction

Osteoporosis is among the most severe problems affecting the quality of life for the elderly. An understanding of the pathophysiology and mechanism of the development of the disease is essential for diagnosis and treatment. Mechanisms of postmenopausal osteoporosis have been studied using animal models and clinical epidemiology or drug testing in human subjects. In contrast, the mechanism of senile osteoporosis has not been well characterized, mainly because of a lack of experimental models. It is generally recognized that senile osteoporosis is characterized by a decrease in bone-forming capacity. Defects in bone formation may be due to a decrease in the number or the function of osteoblasts, or both. Here, we review potential mouse models of senile osteoporosis with focus on osteoblastic function.

Offprint requests to: K. Watanabe
(e-mail: kwatanab@nils. go.jp)
Received: April 30, 2004 / Accepted: April 30, 2004
* Recipient of JSBMR Encouragement Award 2002

Proliferation and differentiation of osteoblasts

To date, important genes for bone development, such as Runx2 and Osterix, have been identified [1–3]. These transcription factors play key roles in osteoblast differentiation [3,4]. Differentiation and maturation of osteoblasts consist of a multistep sequence (Fig. 1). Osteoblasts are thought to derive from mesenchymal stem cells (MSCs), as are other lineages such as myocytes and adipocytes [5]. MSCs self-renew within an appropriate niche, maintaining their pluripotency. This first step (step I, Fig. 1) is critical for tissue maintenance, metabolism, and regeneration and is thought to be sensitive to aging. Once leaving the niche, MSCs start differentiation by responding to a variety of signals such as cytokines, hormones, adhesion molecules, or the extracellular matrix (ECM). Bone morphogenetic proteins (BMPs) are well known to induce ectopic bone formation and to accelerate osteoblastic differentiation, but BMPs also regulate development and regeneration of tissues other than bone [6]. For example, BMP can induce adipogenesis of stromal cell lines in vitro [7,8]. IL-1 signaling through the TAK1/TAB1/NIK pathway inhibits peroxisome proliferator-activated receptor γ (PPARγ) function, resulting in suppression of adipogenesis and a switch to osteoblastic differentiation [9]. Thus, many factors converge on osteoblastic differentiation cooperatively or antagonistically. When regulatory mechanisms in this second step (step II, Fig. 1) fail, osteoblastic differentiation is impaired, concomitantly with hypo- or hyperinduction of other lineages.

"Matching of seeds and soil" is an essential step in osteoblastic differentiation. Osteoblasts produce a large amount of collagens and other ECM molecules to build bone while sensing the matrix to stimulate osteoblastogenesis. A mitogen-activated protein (MAP) kinase, extracellular signal-regulated kinase (ERK), responds to extracellular signals and phosphorylates RUNX2, which is known to regulate genes encoding ECM mol-

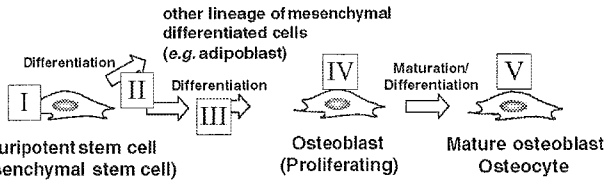

Fig. 1. Multistep differentiation of osteoblast lineage. The process of osteoblastic differentiation can be divided into five regulatory steps. The first step (*I*) corresponds to pluripotent mesenchymal stem cells in the stem cell niche as a source of osteoblasts. In the second step (*II*), lineage selection takes place. Commitment to osteoblastic differentiation is completed, and a checkpoint for progress in maturation may occur at step *III*. Step *IV* corresponds to osteoblast proliferation and activation of mature osteoblasts, e.g., responding to mechanical stress. The last decision as to whether osteoblasts undergo terminal differentiation into osteocytes or apoptosis is made at step *V*

ecules, to activate its transcriptional function [10,11]. This positive feedback step (step III, Fig. 1) may be one of the checkpoints for proceeding to osteoblastic differentiation before deposition of minerals.

Many stimuli have been reported to activate osteoblastic proliferation. Among the most recognized molecules that increase the number of osteoblasts are insulin-like growth factors (IGFs) [12,13]. The Wnt pathway, as a signal that stimulates proliferation, is another candidate [14–16]. Although the authentic ligand that activates the receptor on osteoblasts has not been identified, the coreceptor, LRP5, plays an essential role in bone formation and in controlling the number of osteoblasts [14–16]. Cyclin D1, one of the most potent mitogenic molecules, is a well-known downstream effector of β-catenin, which is a signal mediator in the canonical pathway of Wnt signaling [17], suggesting that Wnt/β-catenin is a pathway leading to increased numbers of osteoblasts and stimulated bone formation.

In the last step shown in Fig. 1, osteoblast differentiation is completed. At this step, osteoblasts produce molecules that regulate mineralization, such as osteocalcin, and release matrix vesicles [18]. Composition of phospholipids also changes in this step, suggesting that lipid metabolism is involved in mineralization [19]. This window may also determine whether osteoblasts undergo apoptosis or terminally differentiate into osteocytes. Although osteoblasts in this step are important for bone quality [20], the mechanism of mineralization or terminal differentiation is largely unknown.

Knockout mice for signaling molecules

As already described, a number of signals are involved in the regulation of osteoblast differentiation. Here, the focus is on genetically modified mouse models showing impaired bone formation. It has been demonstrated that Sca-1, a cell-surface molecule that is expressed in hematopoietic stem cells, is required to maintain self-renewal of mesenchymal stem cells during step I [21]. Sca-1 knockout (KO) mice develop bone normally, but bone mass decreases as they age [21]. IRS-1, a major substrate of insulin receptor (IR) and IGF-1 receptor (IGF-1R) that transduces signals by interacting signaling molecules in a phosphorylation-dependent manner, is expressed in osteoblasts but not in osteoclasts [22]. IRS-1 KO mice exhibit low bone mass compared with controls, and cultured osteoblasts from KO mice are impaired in IGF-induced proliferation and differentiation, whereas differentiation induced by BMP is not altered [22]. In contrast, BMP-induced differentiation was markedly lowered in osteoblasts from Abl KO mice, which are osteopenic due to decreased bone formation [23]. ABL is known as a downstream mediator of integrin signaling, and may function during step III integrating signals from BMP and ECM.

Proliferation of osteoblasts is also impaired in Abl KO mice [23]. LRP5 KO has been reported as a model for osteoporosis and pseudoglioma syndrome, pointing to the involvement of Wnt signaling [24]. Those defects are mainly in the osteoblastic lineage, but do not have a cell-autonomous effect in osteoclastogenesis. On the other hand, knockout mice for another insulin substrate, IRS-2, also showed an osteopenic phenotype with reduced bone formation and accelerated bone resorption [25]. Osteoblasts from IRS-2 KO mice exhibit impaired differentiation but possess accelerated osteoclastogenesis-supporting activity with increased expression of RANKL. This model may serve as an "uncoupling" phenomenon of bone formation and resorption [25]. In view of the unexpected finding of increased bone mass in calcitonin (CT) KO mice, CT may have antibone formation activity in vivo despite the fact that it has long been thought to have antiresorptive activity [26]. It would be interesting to elucidate CT signaling on osteoblasts in relation to parathyroid hormone (PTH) signaling, both of which transduce signals through the G-protein-coupled receptor. In most cases, the development of new anabolic drugs depends on a priori clarification of the means by which these signals regulate bone formation.

Mouse models for premature aging syndromes

Human progeroid syndromes include genetic diseases such as the Werner, Cockayne, and Hutchinson–Gilford syndromes, for which responsible genes are involved in maintenance of genomic stability. Mice with mutations of the responsible genes have not always shown the

expected aging phenotype [27]. However, most of these mice exhibit osteopenia as a hallmark of the pathology. Contrary to expectations, mice deficient in Werner syndrome helicase (WRN) or telomerase RNA component (mTR) did not show signs of accelerated aging, and this may be due to the difference in telomere length between humans and mice [28,29]. Evidently, the phenotype of premature aging develops after four generations in mTR KO mice [30]. It is possible that WRN KO mice may also exhibit an aging phenotype once their telomere length becomes critically short.

Although a classic model of senescence-accelerated mouse (SAM)-P6 is known to show osteopenia, the responsible gene(s) have not been identified [31]. Mice expressing mutant p53 proteins exhibit premature aging [32,33]. In mice expressing the N-terminally deleted p24 isoform or A135V mutant protein of p53, the osteopenic lesion is significant, with the result that both bone formation and resorption are greatly suppressed in these mice [32]. Klotho mice, which are produced by inactivation of the kl gene, exhibit a variety of age-related symptoms, and represent the first established case in which the gene encodes an extracellular protein rather than a nuclear molecule [34]. The pathogenesis of low-turnover osteopenia in the klotho mouse is well documented, resulting in a substantial decrease in osteoprogenitor pools [35]. A knockout mouse for the ataxia telangiectasia mutated (ATM) gene is also recognized as a model of premature aging, and shows a severe osteopenic phenotype with decreased bone formation [36].

It has been reported that IGFs inhibit p53 function by destabilizing the protein [37]. Interestingly, IGF-1R is downregulated in cells from ATM patients as well as those from ATM KO mice [36,38]. Loss of function of IRS-1 and IRS-2 leads to reduced bone formation [22,25]. Transgenic mice expressing IGF-1 in osteoblasts exhibit increased bone mass [39]. Although dysregulation of renal phosphate handling has been reported in klotho mice [40], bone formation seems to be resistant to growth hormone (GH) treatment [41]. It might be interesting to see whether the kl gene is involved in IGF signaling.

Defects in osteoblasts of these animals are often associated with a decrease in the number of osteoclasts as well as reduced hematopoiesis in bone marrow. It has been recently demonstrated that osteoblasts provide a stem cell niche in bone marrow [42,43]. This finding is in good agreement with the cell biological basis of low turnover as represented in klotho, ATMKO, and Sca1KO, but not only in relationship to osteoclastogenesis. Thus, failure in the maintenance of stem cell niche may underlie the pathogenesis of senile osteoporosis.

Is strong bone contrary to longevity?

Although the importance of IGF in bone is evident, IGF signaling does not favor long life span, at least in experimental animals [44]. Caloric restriction (CR) is the only established strategy that can prolong life span in various organisms spanning in diversity from yeast to mammals [45]. Decreased levels in growth hormone and insulin, as well as IGF-1, have been reported in CR animals. Mice defective in the GH–IGF axis or insulin signaling also showed expanded life span. Thus, there may exist a trade-off between longevity and strong bone. Is thicker bone contrary to longevity? Transgenic mice that express the p44 isoform of p53 exhibit an accelerated aging phenotype and short life span [33]. These mice showed decreased BMD, and histomorphometric analysis indicated a low turnover state of bone metabolism. In cells or tissues from the p44 mice, downregulation of phosphatase and tensin homologue deleted on chromosome 10 (PTEN) function and an increased level of phosphorylated Akt were observed, suggesting that hyperactivation of IGF signaling may occur [33]. This observation is in agreement with the GH/insulin/IGF hypothesis on longevity, but does not indicate exerting a favorable action on bone formation. Although it remains to be clarified whether IGF signaling is also hyperactive in the bones, it is suggested that tissue- or stage ('step' in osteoblast lineage)-specific response, or local feedback of IGF, needs to be considered in the action of the growth factor in bone formation.

Aging is a complex, unavoidable phenomenon, and many factors, not only genetic but also environmental, are involved. In terms of age-related changes in bone metabolism, we have to pay attention to neural control of bone formation [46] and consider age-related decline in mechanical stress response and mineral homeostasis by the kidney and/or intestine. Although we should recognize pathophysiological or structural differences between mouse and human skeletons, model mice provided valuable lessons that are useful for elucidating the etiology of senile osteoporosis.

Acknowledgments. We are grateful to Dr. Kyoji Ikeda (NCGG) for helpful discussion and advice. This study was supported in part by the Program for Promotion of Fundamental Studies in Health Sciences of the Organization for Pharmaceutical Safety and Research of Japan.

References

1. Komori T, Yagi H, Nomura S, Yamaguchi A, Sasaki K, Deguchi K, Shimizu Y, Bronson RT, Gao YH, Inada M, Sato M, Okamoto R, Kitamura Y, Yoshiki S, Kishimoto T (1997) Targeted disruption of Cbfa1 results in a complete lack of bone formation owing to maturational arrest of osteoblasts. Cell 89:755–764
2. Otto F, Thornell AP, Crompton T, Denzel A, Gilmour KC, Rosewell IR, Stamp GW, Beddington RS, Mundlos S, Olsen BR,

Selby PB, Owen MJ (1997) Cbfa1, a candidate gene for cleidocranial dysplasia syndrome, is essential for osteoblast differentiation and bone development. Cell 89:765–771
3. Nakashima K, Zhou X, Kunkel G, Zhang Z, Deng JM, Behringer RR, de Crombrugghe B (2002) The novel zinc finger-containing transcription factor osterix is required for osteoblast differentiation and bone formation. Cell 108:17–29
4. Ducy P, Zhang R, Geoffroy V, Ridall AL, Karsenty G (1997) Osf2/Cbfa1: a transcriptional activator of osteoblast differentiation. Cell 89:747–754
5. Prockop DJ (1997) Marrow stromal cells as stem cells for nonhematopoietic tissues. Science 276:71–74
6. Reddi AH (1997) Bone morphogenetic proteins: an unconventional approach to isolation of first mammalian morphogens. Cytokine Growth Factor Rev 8:11–20
7. Ahrens M, Ankenbauer T, Schroder D, Hollnagel A, Mayer H, Gross G (1993) Expression of human bone morphogenetic proteins-2 or -4 in murine mesenchymal progenitor C3H10T1/2 cells induces differentiation into distinct mesenchymal cell lineages. DNA Cell Biol 12:871–880
8. Chen D, Ji X, Harris MA, Feng JQ, Karsenty G, Celeste AJ, Rosen V, Mundy GR, Harris SE (1998) Differential roles for bone morphogenetic protein (BMP) receptor type IB and IA in differentiation and specification of mesenchymal precursor cells to osteoblast and adipocyte lineages. J Cell Biol 142:295–305
9. Suzawa M, Takada I, Yanagisawa J, Ohtake F, Ogawa S, Yamauchi T, Kadowaki T, Takeuchi Y, Shibuya H, Gotoh Y, Matsumoto K, Kato S (2003) Cytokines suppress adipogenesis and PPAR-gamma function through the TAK1/TAB1/NIK cascade. Nat Cell Biol 5:224–230
10. Xiao G, Wang D, Benson MD, Karsenty G, Franceschi RT (1998) Role of the alpha2-integrin in osteoblast-specific gene expression and activation of the Osf2 transcription factor. J Biol Chem 273:32988–32994
11. Xiao G, Jiang D, Thomas P, Benson MD, Guan K, Karsenty G, Franceschi RT (2000) MAPK pathways activate and phosphorylate the osteoblast-specific transcription factor, Cbfa1. J Biol Chem 275:4453–4459
12. Delany AM, Pash JM, Canalis E (1994) Cellular and clinical perspectives on skeletal insulin-like growth factor I. J Cell Biochem 55:328–333
13. Marie P (1997) Growth factors and bone formation in osteoporosis: roles for IGF-I and TGF-beta. Rev Rheum Engl Ed 64:44–53
14. Little RD, Carulli JP, Del Mastro RG, Dupuis J, Osborne M, et al. (2002) A mutation in the LDL receptor-related protein 5 gene results in the autosomal dominant high-bone-mass trait. Am J Hum Genet 70:11–19
15. Gong Y, Slee RB, Fukai N, Rawadi G, Roman-Roman S, et al. (2001) LDL receptor-related protein 5 (LRP5) affects bone accrual and eye development. Cell 107:513–523
16. Boyden LM, Mao J, Belsky J, Mitzner L, Farhi A, Mitnick MA, Wu D, Insogna K, Lifton RP (2002) High bone density due to a mutation in LDL-receptor-related protein 5. N Engl J Med 346:1513–1521
17. Shtutman M, Zhurinsky J, Simcha I, Albanese C, D'Amico M, Pestell R, Ben-Ze'ev A (1999) The cyclin D1 gene is a target of the beta-catenin/LEF-1 pathway. Proc Natl Acad Sci U S A 96:5522–5527
18. Ecarot-Charrier B, Glorieux FH, van der Rest M, Pereira G (1983) Osteoblasts isolated from mouse calvaria initiate matrix mineralization in culture. J Cell Biol 96:639–643
19. Haining SA, Galloway JH, Brown BL, Guilland-Cumming DF (1988) Action of 1,25-dihydroxyvitamin D3 on phospholipid metabolism of human bone cells in culture. J Endocrinol 116:435–441
20. Ducy P, Desbois C, Boyce B, Pinero G, Story B, Dunstan C, Smith E, Bonadio J, Goldstein S, Gundberg C, Bradley A, Karsenty G (1996) Increased bone formation in osteocalcin-deficient mice. Nature (Lond) 382:448–452
21. Bonyadi M, Waldman SD, Liu D, Aubin JE, Grynpas MD, Stanford WL (2003) Mesenchymal progenitor self-renewal deficiency leads to age-dependent osteoporosis in Sca-1/Ly-6A null mice. Proc Natl Acad Sci U S A 100:5840–5845
22. Ogata N, Chikazu D, Kubota N, Terauchi Y, Tobe K, Azuma Y, Ohta T, Kadowaki T, Nakamura K, Kawaguchi H (2000) Insulin receptor substrate-1 in osteoblast is indispensable for maintaining bone turnover. J Clin Invest 105:935–943
23. Li B, Boast S, de los Santos K, Schieren I, Quiroz M, Teitelbaum SL, Tondravi MM, Goff SP (2000) Mice deficient in Abl are osteoporotic and have defects in osteoblast maturation. Nat Genet 24:304–308
24. Kato M, Patel MS, Levasseur R, Lobov I, Chang BH, Glass DA II, Hartmann C, Li L, Hwang TH, Brayton CF, Lang RA, Karsenty G, Chan L (2002) Cbfa1-independent decrease in osteoblast proliferation, osteopenia, and persistent embryonic eye vascularization in mice deficient in Lrp5, a Wnt coreceptor. J Cell Biol 157:303–314
25. Akune T, Ogata N, Hoshi K, Kubota N, Terauchi Y, Tobe K, Takagi H, Azuma Y, Kadowaki T, Nakamura K, Kawaguchi H (2002) Insulin receptor substrate-2 maintains predominance of anabolic function over catabolic function of osteoblasts. J Cell Biol 159:147–156
26. Hoff AO, Catala-Lehnen P, Thomas PM, Priemel M, Rueger JM, Nasonkin I, Bradley A, Hughes MR, Ordonez N, Cote GJ, Amling M, Gagel RF (2002) Increased bone mass is an unexpected phenotype associated with deletion of the calcitonin gene. J Clin Invest 110:1849–1857
27. Hasty P, Campisi J, Hoeijmakers J, van Steeg H, Vijg J (2003) Aging and genome maintenance: lessons from the mouse? Science 299:1355–1359
28. Lebel M, Leder P (1998) A deletion within the murine Werner syndrome helicase induces sensitivity to inhibitors of topoisomerase and loss of cellular proliferative capacity. Proc Natl Acad Sci U S A 95:13097–13102
29. Lee HW, Blasco MA, Gottlieb GJ, Horner JW II, Greider CW, DePinho RA (1998) Essential role of mouse telomerase in highly proliferative organs. Nature (Lond) 392:569–574
30. Rudolph KL, Chang S, Lee HW, Blasco M, Gottlieb GJ, Greider C, DePinho RA (1999) Longevity, stress response, and cancer in aging telomerase-deficient mice. Cell 96:701–712
31. Takeda T, Matsushita T, Kurozumi M, Takemura K, Higuchi K, Hosokawa M (1997) Pathobiology of the senescence-accelerated mouse (SAM). Exp Gerontol 32:117–127
32. Tyner SD, Venkatachalam S, Choi J, Jones S, Ghebranious N, Igelmann H, Lu X, Soron G, Cooper B, Brayton C, Hee Park S, Thompson T, Karsenty G, Bradley A, Donehower LA (2002) p53 mutant mice that display early ageing-associated phenotypes. Nature (Lond) 415:45–53
33. Maier B, Gluba W, Bernier B, Turner T, Mohammad K, Guise T, Sutherland A, Thorner M, Scrable H (2004) Modulation of mammalian life span by the short isoform of p53. Genes Dev 18:306–319
34. Kuro-o M, Matsumura Y, Aizawa H, Kawaguchi H, Suga T, Utsugi T, Ohyama Y, Kurabayashi M, Kaname T, Kume E, Iwasaki H, Iida A, Shiraki-Iida T, Nishikawa S, Nagai R, Nabeshima YI (1997) Mutation of the mouse klotho gene leads to a syndrome resembling ageing. Nature (Lond) 390:45–51
35. Kawaguchi H, Manabe N, Miyaura C, Chikuda H, Nakamura K, Kuro-o M (1999) Independent impairment of osteoblast and osteoclast differentiation in klotho mouse exhibiting low-turnover osteopenia. J Clin Invest 104:229–237
36. Hishiya A, Ito M, Ikeda K, Watanabe K (2002) Decreased bone formation in ataxia telangiectasia mutated (ATM) knockout mice. J Bone Miner Res 17:S299
37. Heron-Milhavet L, LeRoith D (2002) Insulin-like growth factor I induces MDM2-dependent degradation of p53 via the p38 MAPK pathway in response to DNA damage. J Biol Chem 277:15600–15606

38. Peretz S, Jensen R, Baserga R, Glazer PM (2001) ATM-dependent expression of the insulin-like growth factor-I receptor in a pathway regulating radiation response. Proc Natl Acad Sci U S A 98:1676–1681
39. Zhao G, Monier-Faugere MC, Langub MC, Geng Z, Nakayama T, Pike JW, Chernausek SD, Rosen CJ, Donahue LR, Malluche HH, Fagin JA, Clemens TL (2000) Targeted overexpression of insulin-like growth factor I to osteoblasts of transgenic mice: increased trabecular bone volume without increased osteoblast proliferation. Endocrinology 141:2674–2682
40. Yoshida T, Fujimori T, Nabeshima Y (2002) Mediation of unusually high concentrations of 1,25-dihydroxyvitamin D in homozygous klotho mutant mice by increased expression of renal 1-alpha-hydroxylase gene. Endocrinology 143:683–689
41. Kashimada K, Yamashita T, Tsuji K, Nifuji A, Mizutani S, Nabeshima Y, Noda M (2002) Defects in growth and bone metabolism in klotho mutant mice are resistant to GH treatment. J Endocrinol 174:403–410
42. Zhang J, Niu C, Ye L, Huang H, He X, Tong WG, Ross J, Haug J, Johnson T, Feng JQ, Harris S, Wiedemann LM, Mishina Y, Li L (2003) Identification of the haematopoietic stem cell niche and control of the niche size. Nature (Lond) 425:836–841
43. Calvi LM, Adams GB, Weibrecht KW, Weber JM, Olson DP, Knight MC, Martin RP, Schipani E, Divieti P, Bringhurst FR, Milner LA, Kronenberg HM, Scadden DT (2003) Osteoblastic cells regulate the haematopoietic stem cell niche. Nature (Lond) 425:841–846
44. Tatar M, Bartke A, Antebi A (2003) The endocrine regulation of aging by insulin-like signals. Science 299:1346–1351
45. Koubova J, Guarente L (2003) How does calorie restriction work? Genes Dev 17:313–321
46. Takeda S, Elefteriou F, Levasseur R, Liu X, Zhao L, Parker KL, Armstrong D, Ducy P, Karsenty G (2002) Leptin regulates bone formation via the sympathetic nervous system. Cell 111:305–317

Available online at www.sciencedirect.com
SCIENCE DIRECT®
Molecular Aspects of Medicine 26 (2005) 221–231
MOLECULAR ASPECTS OF MEDICINE
www.elsevier.com/locate/mam

Review

Mouse models of senile osteoporosis

Ken Watanabe *, Akinori Hishiya

Department of Bone & Joint Disease, National Center for Geriatrics & Gerontology (NCGG), Aichi 474-8522, Japan

Special issue for "molecular mechanisms of aging bone"

Abstract

Little is known about the pathophysiology of normal human and mouse senescence. On the other hand, the pathology of age-related disorders, such as senile osteoporosis, has been investigated. In vivo studies on the pathology of osteoporosis have been conducted primarily in rodents. Although mouse models of senile osteoporosis display some discrepancies relative to their human counterparts with regard to symptoms and pathology, these experimental models are useful and powerful tools for basic and preclinical studies. Here, we review existing mouse models of senile osteoporosis, including those exhibiting premature aging phenotypes, and discuss their pathogenesis, particularly with regard to age-related changes in stem cells.

Keywords: Premature aging; Senile osteoporosis; Stem cell; Osteoblast

Contents

1. Classical models for senile osteoporosis 222
2. Premature aging syndromes in genetically modified mice 223
3. Bone formation defects mimicking pathogenesis in senile osteoporosis 226

* Corresponding author. Tel.: +81 562 46 2311; fax: +81 562 44 6595.
E-mail address: kwatanab@nils.go.jp (K. Watanabe).

0098-2997/$ - see front matter
doi:10.1016/j.mam.2005.01.006

4. Concluding remarks 227
Acknowledgments 228
References 228

1. Classical models for senile osteoporosis

A decrease in bone mass accompanying advancing age is not specific to humans, but has also been observed in other mammals. Laboratory mice usually live for 2–3 years, and show a peak bone mass at 4–8 months of age, followed by a decline with advanced age. A popular laboratory mouse strain, C57BL/6, develops a senile osteoporosis-like bone phenotype with decreased bone mass and quality (Perkins et al., 1994; Bikle et al., 2002; Cao et al., 2003; Ferguson et al., 2003). Both trabecular and cortical bones suffer dynamic changes with age in this model. Whereas the cancellous bone volume fraction (BV/TV) is significantly decreased from ages 6 weeks to 24 months, cortical thickness is increased until the age of peak bone mass (~6 months), after which it subsequently declines (Bikle et al., 2002). Interestingly, expression of RANKL, also known as osteoclast differentiation factor, is increased with age, correlating with cancellous bone volume (Cao et al., 2003). In another common mouse strain, BALB/c, osteogenic stem cells from 24-month old mice exhibit a decrease in proliferative potential upon aging (Bergman et al., 1996). It is suggested that this age-related bone loss is caused by decreased osteogenic potential due to both quantitative and qualitative declines, especially in stem cell function (Bergman et al., 1996). Additionally, bone marrow hematopoiesis is often affected by aging (Morrison et al., 1996). C57BL/6 mice are known to frequently develop clonal B cell expansion and lymphoma with advanced age (LeMaoult et al., 1999; Ghia et al., 2000). This raises the possibility that age-related, strain-specific hematopoietic disorganization, such as that observed in lymphoma, largely affects bone resorption.

Senescence accelerated mice (SAM) have been established by Takeda et al., and accepted as an appropriate model of aging (Takeda et al., 1997). The SAM lines, derived from the mouse strain, AKR/J, are divided into two classes; P lines exhibit an accelerated aging phenotype with shortened life-span, and R lines show a relatively less accelerated phenotype. The aging phenotype of P lines becomes apparent at 6–8 months of age. Among the SAM lines, SAM-P6 has been utilized as a model for human senile osteoporosis, and characterization of the resultant bone phenotype has been well described (Matsushita et al., 1986; Jilka et al., 1996; Kajkenova et al., 1997; Silva et al., 2002). Jilka et al. (1996) demonstrated that the osteopenic phenotype was caused by reduced osteoblastogenesis and that bone metabolism was resistant to gonadectomy. Furthermore, increased adipogenesis and myelopoiesis have been observed in bone marrow from the mice (Kajkenova et al., 1997). In addition, the long bones in SAM-P6 were longer but more fragile than those in controls (Silva et al., 2002). With these and other numerous reports of in vivo and ex vivo studies with the SAM-P6 model, a number of phenotypic characteristics, thought to be consistent between aging mice and humans, have been observed. It should be noted,